Tharaneedhar Varadarajan

Hydraulic Scale Modelling of Pressurized Sand Traps

Master's thesis in Hydropower Development
Supervisor: Kaspar Vereide
Co-supervisor: Leif Lia, Ola Haugen Havrevoll
June 2024

Master's thesis

NTNU
Norwegian University of Science and Technology
Faculty of Engineering
Department of Civil and Environmental Engineering

NTNU
Norwegian University of
Science and Technology

Tharaneedhar Varadarajan

Hydraulic Scale Modelling of Pressurized Sand Traps

Master’s thesis in Hydropower Development
Supervisor: Kaspar Vereide
Co-supervisor: Leif Lia, Ola Haugen Havrevoll
June 2024

Norwegian University of Science and Technology
Faculty of Engineering
Department of Civil and Environmental Engineering

NTNU
Norwegian University of
Science and Technology

M.Sc. THESIS IN HYDRAULIC ENGINEERING

Candidate: Mr. Tharaneedhar Varadarajan

Title: Hydraulic Scale Modelling of Pressurized Sand Traps

1. Background

In Norway and many countries in Europe, installation of unregulated power sources such as solar power and wind power will increase in the years to come. This may result in upgrading of existing hydropower plants for purposes including production of peak power and balancing of energy production.

The current power prices make it profitable to upgrade the installed capacity in existing hydropower plants. There is already a number of large hydropower plants that have been upgraded with a higher installed capacity. Several of these upgraded hydropower plants have experience problems with sand that has caused damage to the turbines after the upgrading. The reason is believed to be that the original sand traps are not functioning as intended after the upgrade.

With this background, much research has been initiated to improve and retrofit the design of pressurized sandtraps in hydropower plants at NTNU. Hydraulic scale models have been central to the research. However, questions have been raised about the accuracy of the hydraulic scale models. Different model scaling laws are available that give different results.

Now, a "model family" consisting of several hydraulic scale models have been constructed at the Norwegian University of Science and Technology (NTNU). The models will be used to study the hydraulic design of sand traps in hydropower plants, and are in scales from 1:100 to 1:20 of a sand trap in the 960 MW Tonstad hydropower plants. The main scope of the model tests is to study the scaling laws and scaling methodology.

Specifically, this project will investigate the effect of two variables:

1. Inclination of the pressurized sand trap invert.
2. Roughness of the pressurized sand trap walls.

The effect shall be quantified in terms of trap efficiency of the sand trap.

3. Main questions for the thesis

The thesis shall cover, though not necessarily be limited to the main questions listed below.

2.1 Literature and desk study

The candidate shall carry out a literature study of design of pressurized sand traps and hydraulic scale model tests of pressurized sediment laden flow.

2.2 Main tasks

The candidate must collect available background material such as reports, operational data, former studies, maps and drawings of the prototype Tonstad hydropower plant and the hydraulic scale models. Related to this material the following must be carried out:

1 Set up an experimental plan
2 Prepare the physical model
3 Testing in the hydraulic scale model
4 Document the results and compare the different results
5 Propose the optimum design of pressurized sand traps in terms of inclination and roughness
6 Conclusions
7 Proposals for future work
8 Presentation

3 Supervision and data input

Adjunct Associate Professor Kaspar Vereide will be the main supervisor. Professor Leif Lia and PhD Candidate Ola Haugen Havrevoll will be co-supervisors. The supervisors shall assist the candidate, and make relevant information available.

Discussion with and input from colleagues and other research or engineering staff at NTNU is recommended. Significant inputs from other shall be referenced in a convenient manner.

The research and engineering work carried out by the candidate relating to this thesis shall remain within an educational context. The candidate and the supervisors are free to introduce assumptions and limitations which may be considered unrealistic or inappropriate in a contract research or a professional/commercial context.

4 Report format and reference statement

The report should be written with a text editing software, and figures, tables, photos etc. should be of good quality. The report should contain an executive summary, a table of content, a list of figures and tables, a list of references and information about other relevant sources. The report should be submitted electronically in B5-format pdf-file.

The executive summary should not exceed 450 words, and should be suitable for electronic reporting. The Master's thesis should be submitted within 10th of June 2024.

Trondheim, 15. January 2024

Kaspar Vereide
Adjunct Associate Professor
Department of Civil and Environmental Engineering
NTNU

Acknowledgment

I would like to express my deepest gratitude to Adjunct Associate Professor Kaspar Vereide Department of Civil and Environmental Engineering, Norwegian Institute of Science and Technology (NTNU) for giving me this opportunity. His constant support and guidance helped me to successfully finish this thesis. I would like to thank Sira-Kvina company for this wonderful opportunity. I would also like to thank the Faculty of Civil and Environmental Engineering of NTNU, Trondheim for offering a fabulous environment to conduct research. This helped me to bring my true potential and upskill myself. I am grateful for the support from Pritam Bogati (master's student). I would like to extend my thanks to PhD candidates Siraq and Kale for their greatest support in the lab. I am very grateful to Eirik and other lab technicians for assisting me in the lab. Many thanks to all my professors and faculties.

My deepest thanks to my wife who is the pillar of support during all this time. Without her mental support, I wouldn't have finished this thesis on time. Many thanks to my family, friends, and God.

Abstract

Hydropower plants have been majorly facing challenges with sediments for decades. If these sediments enter the turbines through various sources, it can cause serious damage to the turbine. This may lead to reduced power production accompanied by economic losses. There are several solutions available to handle these sediments. One of the solutions is the closed sand trap. Based on recent research, the implementation of ribs and ramp structure in the closed sand trap shows improved trap efficiency. This thesis focuses on testing the hydraulic scale modeling of pressurized sand traps with ribs and ramp structure and examines how various slope conditions and roughness levels affect trap efficiency. Sand trap no. 3 of the Tonstad power plant have been taken as prototype. Physical models are made with scale ratios of 1:100 and 1:200. They are used to study the trap efficiency under different slopes and roughness conditions.

Based on the results obtained, plexiglass roughness with a declined slope (4°) in the 1:100 scale models have the maximum efficiency (76.2%), whereas sandpaper roughness under the same slope produces the lowest efficiency (66.8%). In the 1:200 scale models, plexiglass roughness shows the highest efficiency of 21.9%, and inclined slopes (4°) have high efficiencies regardless of roughness conditions. This shows that the smooth roughness conditions aid in achieving higher trap efficiency, but more investigation is needed to determine the optimal slope conditions to achieve higher trap efficiency.

Sammendrag

Vannkraftverk har i flere tiår hatt store utfordringer med sedimenter. Hvis disse sedimentene kommer inn i turbinene via ulike kilder, kan det føre til alvorlige skader på turbinen. Dette kan resultere i redusert kraftproduksjon og økonomiske tap. Det finnes flere løsninger for å håndtere disse sedimentene. En av løsningene er den lukkede sandfangeren. Basert på nyere forskning viser implementering av ribber og ramp-struktur i den lukkede sandfangeren forbedret fangst effektivitet. Denne avhandlingen fokuserer på testing av hydraulisk skalamodellering av trykksatte sandfangere med ribber og ramp-struktur, og vil undersøke hvordan ulike helningsforhold og ruhetsnivåer påvirker fangst effektiviteten. Sandfanger nr. 3 ved Tonstad kraftverk er tatt som prototype. Fysiske modeller er laget med skalaforhold på 1:100 og 1:200. Disse brukes til å studere fangst effektiviteten under forskjellige helnings- og ruhetsforhold.

Basert på resultatene oppnådd, har pleksiglass ruhet med en fallende helning (4°) i 1:100 skalamodellene den maksimale effektiviteten (76,2%), mens sandpapir ruhet under samme helning gir den laveste effektiviteten (66,8%). I 1:200 skalamodellene viser pleksiglass ruhet den høyeste effektiviteten på 21,9%, og skrånende helninger (4°) har effektivitet uansett ruhetsforhold. Dette viser at glatte ruhetsforhold bidrar til å oppnå høyere fangst effektivitet, men mer undersøkelse er nødvendig for å bestemme de optimale helningsforholdene for å oppnå høyere fangst effektivitet.

Contents

List of Figures

List of tables

List of symbols

A	-	Area
a	-	Acceleration
ADCP	-	Acoustic doppler current profiler
CFD	-	Computational Fluid Dynamics
d	-	Diameter
d_{cr}	-	Critical particle size
E	-	Young's modulus
F	-	Froude number
g	-	Acceleration due to gravity
GWh	-	Giga watt-hour
Kg	-	Kilogram
L	-	Characteristic length
m/s	-	Meter per second
m^3	-	Cubic meter
m^3/s	-	Meter cubic per second
mm	-	Millimeter
Mm^3	-	Million-meter cube
MW	-	Mega Watts
P	-	Pressure
PIV	-	Particle image velocimetry

q_{se}	-	Amount of sediments leaving the basin
q_{si}	-	Amount of sediments entering the basin
R_e	-	Reynolds number
R_h	-	Hydraulic radius
S	-	Slope
S_a	-	Arithmetical mean height
S_{ku}	-	Kurtosis
S_p	-	Maximum peak height
S_q	-	Root mean square height
S_{sk}	-	Skewness
S_v	-	Maximum pit height
S_z	-	Maximum height
V	-	characteristic velocity
α	-	Vertical expansion angle
γ	-	Specific weight
ε	-	Absolute roughness
η	-	Trap efficiency
μ	-	Dynamic viscosity
ν	-	Kinematic viscosity
ρ	-	Density
σ	-	surface tension
τ^*	-	Critical shear stress
τ_0	-	Bed shear stress
$d50$	-	Median sediment grain size
ρ_w	-	Density of water
ρ_s	-	Sediment density

1. Introduction

1.1 Background

Alarmed by global warming and climate change, most countries, especially developed nations are switching to renewable energy sources for their power supply. Hydropower is one of the efficient renewable energy sources. Unlike other renewable energy sources which can be utilized only during their periods of availability, hydropower offers the advantage of extended utilization throughout the year by storing water in reservoirs. This allows the regulation of hydropower generation to maintain a consistent power supply. However, the capacity of reservoirs is significantly hindered by the accumulation of sediments from incoming water bodies. One of the best examples is the Binga reservoir in the Philippines, whose capacity has been reduced from 95 Mm^3 in 1960 to 21 Mm^3 in 2015 which is almost a 78% reduction in reservoir capacity (Lal Maskey et al., 2020). These sediments can also enter the hydropower tunnels, passing through the turbines and damaging them. Installation of a desilting basin at the inlet of the tunnel or conduit could be an option to protect turbines. This allows the sediment to settle in the basin and prevents the turbine from damage but most of the Norwegian hydropower system has multiple inlets which makes it impractical and economically less attractive to have a desilting basin at each inlet. Additionally, for economic reasons, most Norwegian hydropower uses unlined tunnel systems due to the quality of the rock. Desilting basins can only trap sediments at the inlet and not the sediments from the tunnel inverts which are left over after construction. To tackle this, a pressurized sand trap that can be constructed on the upstream side of the turbine can eliminate sediments from various sources such as main intakes, brook intakes, and particles from unlined walls (Richter et al., 2021). This in turn protects the turbines from damage.

Despite having pressurized sand traps, power plants equaling 25% of the total installed capacity in Norway have faced sediment issues during operation (Richter et al., 2021). This resulted in problems ranging from minor wear to major turbine damage. The possible reasons for these problems were upgrading of installed capacity leading to more discharge along with more sediments, flexible operations, and climate change followed by intense floods with higher sediment concentration. As the sand traps are underperforming, retrofitting sand traps is required. In terms of retrofitting, there are several feasible options to modify the sand trap such as an expansion of the sand trap area, installation of diffusers, and using flow-calming structures. To implement them, they must be cost-effective, perform well, and have the least downtime. For example, sand trap area expansion is a viable solution but could be costly and time-consuming which might affect production subsequently the investors and owners. Flow-calming structures could be installed but are less effective in trapping sand as they create additional turbulence and allow sand to escape (Richter et al., 2021). Recent research such as (Havrevoll et al., 2021; Ivarson et al., 2021; Richter et al., 2021) shows that a closed sand trap seems to be a promising solution for sediment issues as it shows superior sand trap efficiency compared to open sand traps. Trap efficiency is an important parameter with which we can assess the effectiveness of the sand trap systems. Although several factors affect the trap efficiency, one of the main factors to consider is the roughness of the tunnel invert where the transportation of sediment bed load occurs. This thesis focuses on analyzing the impact of invert roughness over trap efficiency of the closed sand trap with ribs and ramp structure.

1.2 Aim of the research

The main aim of this master's thesis is to determine how the sand trap efficiency is affected by different floor roughness conditions and inclinations and to propose optimal conditions for maximizing sand trap efficiency. This is done by evaluating the scaled models of closed sand traps with ribs and ramp structures under different roughness and slope conditions. Experiments will be conducted for two different roughness conditions for each scale model (1:100 and 1:200). The sand trap no.3 of the Tonstad power plant has been taken as the prototype. The roughness conditions are Plexiglass roughness and sandpaper roughness on the invert. Each roughness condition will be subjected to three different inclination levels (inclined for 4°, parallel to the floor, and declined for 4°). Experiments will be repeated for three times at particular roughness and inclination levels for sensitivity analysis.

Another aim is to evaluate the scaling approaches and determine whether the two scaling factors produce similar results. Experiments will be conducted using scaled models at a 1:100 and 1:200 scale ratio to assess the trap efficiency of the sand traps and compare the same. Water velocity and sand particle sizes have been kept in the ratio of 1:1 between the prototype and the models.

1.3 Research questions and hypothesis

The hypothesis answers the following research questions.

1. Which roughness and slope conditions will have maximum trap efficiency?
2. Will the two scale factors 1:100 and 1:200 in models produce similar results?

The hypothesis for the first question is that the maximum trap efficiency can be witnessed in both scale models which have plexiglass roughness on the invert and have parallel slope. The reason why plexiglass roughness will have maximum trap efficiency compared to sandpaper roughness is that the former condition creates less turbulence which allows more particles to settle inside the sand trap. Unlike the other two slope conditions, the parallel slope will have maximum trap efficiency as it doesn't disturb the natural water flow rhythm. Although an inclination of 4° of invert seems to be a viable option as it resists sand movement by its inclined angle, it might reduce the cross-sectional area of the chamber resulting in increased water velocity. If the velocity is higher than the critical velocity of the sediment particle then the particle will be carried in suspension which might reduce the chance of sand particles getting trapped (Leod et al., n.d.). If the total chamber from the crown till invert is inclined to 4°, then it may lead to more head loss causing other issues. And regarding declination 4°, it might increase the bed load particle velocity due to declined slope and cause particle interaction which might allow the settled particles to suspend and escape.

The hypothesis for the second question is that the results from the 1:100 and 1:200 scale models will not be similar. This is because we're using an unusual scaling method where the velocity and particle size remain constant across both models, similar to the prototype. However, since these models have different geometric sizes, particle behaviour such as transportation rate, settling, and sand trap efficiency is likely to vary, resulting in different outcomes.

1.4 Structure of thesis

This master's thesis is organized into seven chapters. Chapter 1 discusses the importance of hydropower in renewable energy, gives background information on sediments and their effects, and highlights the issues Norwegian hydropower faces due to sediment. It also introduces the work and explains the hypothesis being tested. Chapter 2 reviews the design of pressurized sand traps and tests of hydraulic scale models with sediment-laden flow. Chapter 3 explains about the sources and transportation of sediments and different sand trap layouts and designs. Chapter 4 covers the prototype background, scale model design, materials used, and the experimental plan. Chapter 5 presents the findings and compares the results from different scaled models. Chapter 6 offers conclusions and recommendations for future research.

2. Literature review

Richter et al., (2017) discussed the problems in the sand trap of the Tonstad power plant and proposed corresponding solutions. In 1988, the upgradation of power from 640 to 960 MW took place at Tonstad along with the additional building of a pressure shaft, sand trap and surge tank. The sand traps are designed to trap grains to a minimum of 2.0 mm in diameter. Due to the higher flexibility demand of power, rapid variations in the discharge have occurred. This has caused sediments to flush into turbines. This also caused challenges to the current surge tank design. Also, it is believed that the flow has changed from pressurized to free flow during an event since two turbines were damaged severely. 3D CFD modelling of the affected area such as part of the head race tunnel, surge tank, and sand trap including roughness has been done at a scale of 1:15. Simulation showed that the water jet entering the upstream gate of the sand trap was found to create turbulence for initial 40 m to 50 m which is believed to be the reason for the sand particles to escape. The authors have suggested two solutions: installing diffusers at the upstream end of the sand trap and expanding the sand trap cross-section with a bottom trench to reduce flow velocity. The solution was simulated with 3D CFD modelling and found to be successful as the particle range of 0.31mm to 1.15 mm at the prototype scale settled more efficiently compared. Physical scale model tests have been started at NTNU to validate the results from the CFD simulations.

Ivarson et al., (2021) numerically investigated the effects of the installation of V-shaped rake structures for flow distribution and rib structures for sediment trapping on sand traps using the SAS-SST Turbulence model. The SAS-SST model was used as it was found to perform better than the conventional RANS formulations. A total of "3" three-dimensional models of sand trap-3 at Tonstad powerplant were created using CAD software at a scale of 1:1. Those are 1) Model without upgrades 2) Model upgraded with Ribs at the downstream section of the sand trap and 3) Model upgraded with Ribs at downstream section and V-shaped rakes at the upstream section of the sand trap. All three models are meshed similarly. In all three models, tetrahedral mesh structures were given for diffuser and invert while hexahedral meshes were for simpler geometries (inlet section, tunnel, penstock). Analysis about a total time of 1000 sec with a time step of 0.5 sec has been adopted. The hydraulic representation of the numerical model was validated by comparing it with PIV on a physical scale model and ADCP measurements from the prototype of the sand trap. The results have shown that the model with ribs has higher trap efficiency compared to the model without upgrades and the model with ribs and V-shaped rakes. The underperformance of the model with ribs and rakes is due to the turbulent vortices preventing smaller sediments from settling thus reducing sand trap efficiency.

Vereide et al., (2021) presented a report on flexible sand traps. The flexible sand trap project was a 4-year project to upgrade existing sand traps in hydropower plants. The main challenge with upgrading is the infrastructure size limitation and downtime due to which there will not be any production. The author and team tried to develop a cost-effective design solution to tackle the above problems. Numerical simulation of preliminary concepts and physical modelling of the most promising concepts has been done. Sand trap no. 3 at Tonstad powerplant is used as a case study. Details such as a full 3D scan of a sand trap, Velocity profile measurements using 3 ADCPs, pictures and videos of sand trap operation and trapped material samples have been used to do numerical and physical modelling tests. Numerical simulations identified several modifications that have positive effects on the trap efficiency such as reconstructing sand traps with ribs, installation of flow-calming structures at the inlet, implementing baffle walls with an automatic sluice system and geometrical modifications for turbulence reduction. Physical model tests conducted at TU Graz revealed that adding ribs significantly increased the trap efficiency from 0% to 90% for particle size between 0.3mm to 1mm. However, physical model tests at NTNU with the particle size of d50 equivalent to 3 mm showed indifferent trap efficiency results with or without ribs.

3. Theory

3.1 Sediments sources

Sediment refers to the mixture of organic and inorganic materials. They are mostly composed of gravel, sand, silt, clay, and algae. In Norway, sources of sediment yield of rivers are clay areas, glaciers, mountains, agriculture, and forests where the clay area acts as a major source of sediments while forest being the minimum.

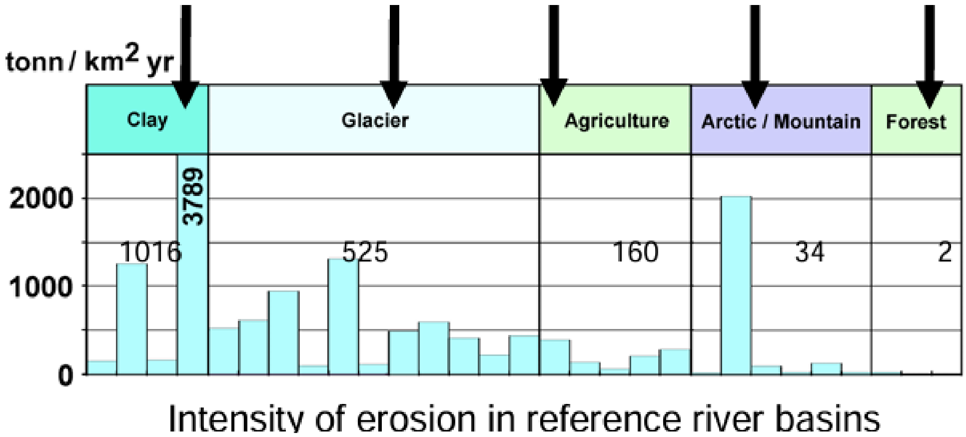

Figure 1 Sediment yield of Norwegian rivers, Norwegian water resources, and energy directorate (2016)

3.2 Sediment transport

Transportation of organic and inorganic particles by water is known as sediment transport. It can also be referred to as sediment load which comprises mainly of Bed load and suspended load as referred to in Figure 2. Bedload refers to coarser material moving along the bed surface by rolling and saltation. Suspended loads are fine materials kept in suspension by water currents. The particle is going to be either a bed load or suspended load depending majorly on the flow rate and size of the particle. But in conventional terms, bed loads are coarser particles (sand, gravel, boulders, etc.,) and suspended loads are finer particles (silt and clay). The particles will be in suspension when the shear velocity is higher than the settling velocity and vice versa.

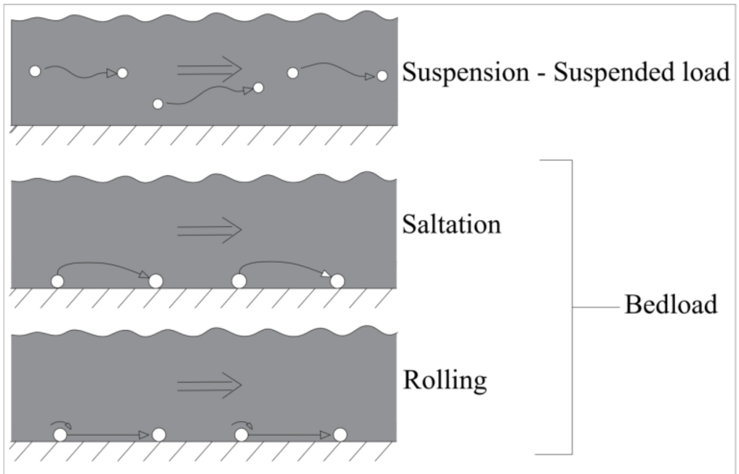

Figure 2 Bed load and Suspended load movement

3.3 Shear stress

Sediment transport and movement of bed load is a function of shear stress. The shear stress is a measure of the frictional force of moving water against the bed of the channel. Different water velocities create different shear forces. When these shear forces act against the bed of a channel, they create shear stress, which initiates the movement of the bedload. The intensity of these stresses depends on the bed slope, channel geometry and flow. They can be expressed as

$$\tau_0 = \rho_w g R_h S \tag{3.1}$$

where, τ_0 is bed shear stress [N/m²], ρ_w is the density of water [kg/m³], g is the acceleration due to gravity [m/s²], R_h is hydraulic radius [m], and S is the slope of energy line [-].

The condition at which the shear forces exceed the restrictive forces (inertia, friction) is called the incipient motion condition where the sediment particle is entrained. The shear stress in this condition is called critical shear stress. This can be determined using the formula provided in the Shields diagram. They can be expressed as

$$\tau^* = \frac{\tau_0}{(\rho_s - \rho) g d_s} \tag{3.2}$$

where τ^* is critical shear stress or critical shield's parameter, τ_0 is bed shear stress [N/m²], ρ_s is the density of sediments [kg/m³], ρ is the density of water [kg/m³], g is the acceleration due to gravity [m/s²], and d_s is the diameter of sediment [m].

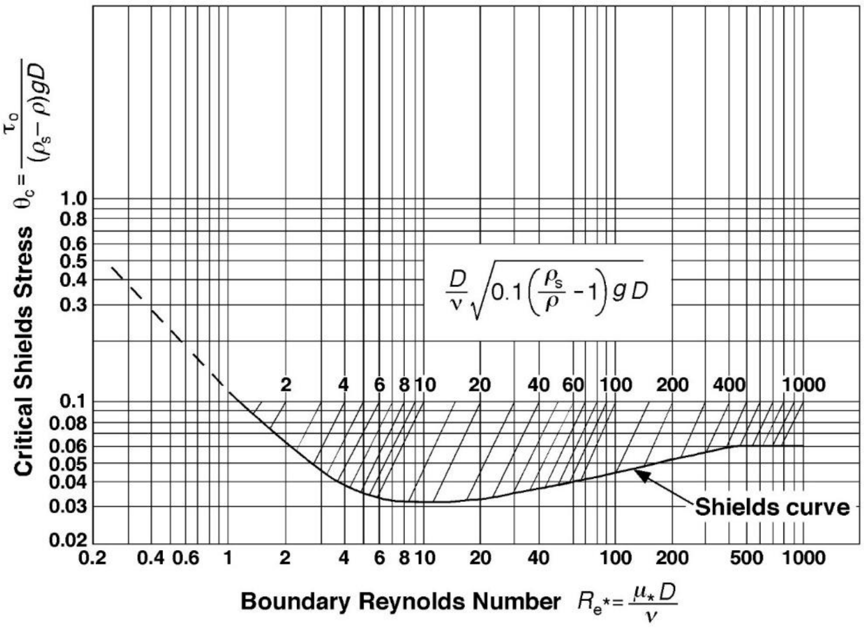

Figure 3 Shield's diagram (Schwimmer, 2013)

3.4 Fluids and particle behavior

Fluid behavior in the water channel can be classified into two types: laminar flow and turbulent flow. The flow is said to be a laminar flow when all the particles and molecules in the fluid move along the flow direction parallel to each other. Whereas in turbulent flow, particles and molecules in fluid move in all directions but with a net movement in a fluid direction. Reynolds number can be used to determine the flow condition.

$$Re = \frac{\rho v D}{\mu} \qquad 3.3$$

Where Re is Reynolds number [-], v is water velocity [m/s], D is conduit diameter [m], μ is dynamic viscosity [$\mathrm{Ns/m^2}$]. The corresponding Table 1 shows different flow conditions and corresponding Reynolds numbers.

Table 1 Reynolds number and Flow conditions

Reynolds number	Flow type
R<2000	Laminar flow
2000<R>4000	Flow transition
R>4000	Turbulent flow

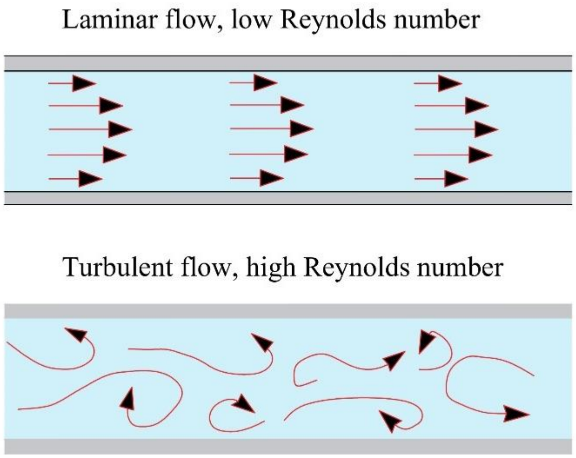

Figure 4 Fluid flow types

This Reynolds number can also be used in the shields diagram (Figure 4) to determine the corresponding critical shield stress with which sediment motion can be assessed.

3.5 Sand trap layout

The sediments passing through the water bodies might enter the tunnels, if not captured could rupture and damage the turbines. Since it is a costlier task to have sand traps at the intake structures for the hydropower with multiple brook intakes, Norwegian sand traps are placed just above the upstream end of the turbines. This placement has the advantage of collecting sediments from all of its sources. The sand traps and turbines are connected by a lined pressure shaft with a surge tank. This design allows the construction of unlined tunnels before the pressure shaft where the construction particles can be left over the invert of the tunnel after construction (Vereide et al., 2017).

The sand traps can be constructed either as open sand traps or closed sand traps as mentioned in the figures below. The main difference between closed and open sand traps lies in their design. The principle of sand trap is to reduce the flow velocity to the lowest allowable magnitude for the longest possible period which results in effective settling of the particles due to gravity. This can be achieved by expanding the cross-sectional area by widening the channel and lowering the floor inside the sand trap (Simanjuntak et al., 2009). Open sand traps operate on the same principle where the expansion from the headrace tunnel is carried out in such a manner to avoid turbulence, flow separation, and resuspension as far as possible.

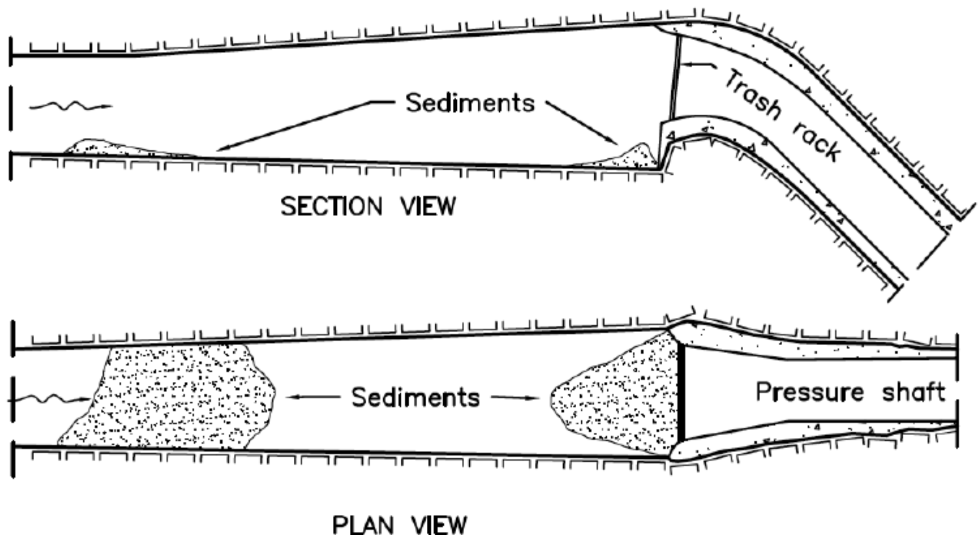

Figure 5 Diagram of an open sand trap with a plan and sectional view (Steinkjer, 2018)

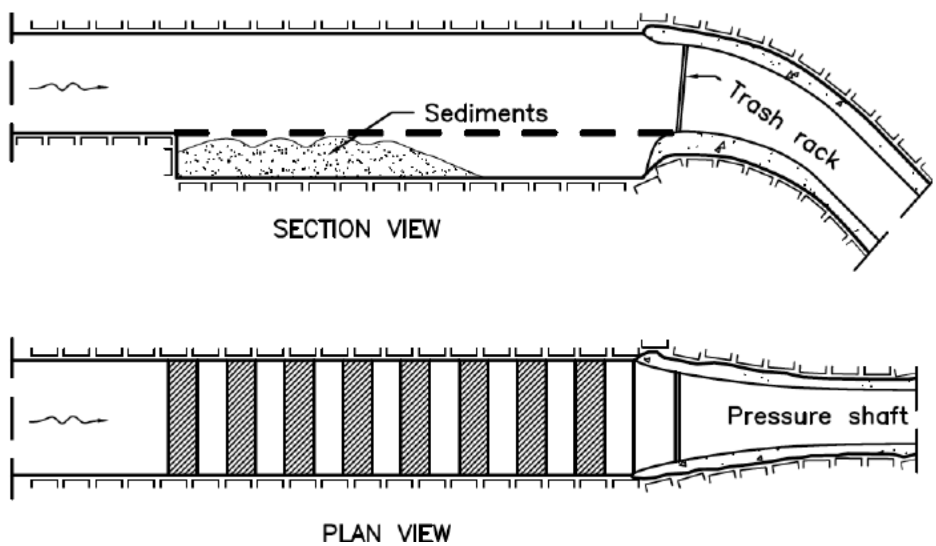

Figure 6 Diagram of a closed sand trap with a plan and sectional view (Steinkjer, 2018)

Closed sand traps are designed with 1 m wide precast concrete ribs with a spacing of 1 m apart from each other. These ribs act as a flow separator between the main flow and the sedimentation pit. Closed sand traps prevent the settled sediments from resuspension. Also, it is less sensitive to non-uniform flow as the separator prevents the turbulence from reaching the sediments. Hence, they can be placed in areas where flow is susceptible to disturbance. Unlike open sand traps, closed sand traps can be constructed without expansion of the flow area. This reduces turbulence which is caused by separation. Although open sand traps are comparatively cheaper than closed sand traps, they have low trap efficiency compared to closed sand traps (Havrevoll et al., 2021).

Sand trap design is not universally the same and differs from country to country. Typical sand trap design is based on the critical particle size where the sediments larger than the same should be removed. Choosing the critical particle size varies for different projects and requires economic optimization. Often sand traps are designed based on experience using general guidelines. In Norway, particles size smaller than 1 – 2mm are generally allowed to pass through the turbines (Vereide et al., 2017).

3.6 Sand trap efficiency

The most important parameter to assess the functionality of the sand trap is the trap efficiency. It shows whether the sand trap performs the intended job by trapping the sand and protecting the turbine from abrasion and damage. Trap efficiency should be fixed at the planning stage, and it depends on turbine abrasion and sand trap cleaning interval. Two commonly used methods to define sand trap efficiency are the critical particle size d_{cr} method, and the sediment mass method. In the critical particle size method, the idea is to design the sand trap to remove the sediments that are larger than the critical particle size. In the sediment mass method, the focus will be emphasized on removing overall sediment concentration. The efficiency is calculated based on the amount of sediments entering and leaving the basin per unit time (Raju et al., 1999) . The corresponding equation can be used to determine the efficiency of the sand trap,

$$\eta = \frac{q_{si} - q_{se}}{q_{si}} \qquad 3.4$$

here η = basin efficiency, q_{si} = amounts of sediment entering the basin per unit time and q_{se} = amounts of sediment leaving the basin per unit time. This master thesis utilizes the above equation to calculate trap efficiency.

4. Methodology

4.1 Prototype description

Tonstad hydropower plant is in Tonstad, a small town in Southern Norway. It has a total installed capacity of 960 MW which accounts for a total of 3800 GWh annual power output. The total head is about 450 meters and has a tunnel system around 30 km in length. It has two intakes and eight secondary brook intakes with an unlined pressurized tunnel system. The power plant was constructed in multiple stages where two turbines of 160 MW were commissioned in 1968 and two more in 1971 which accounts for a total of 640 MW. In 1988, it was upgraded from 640 MW to 960 MW.

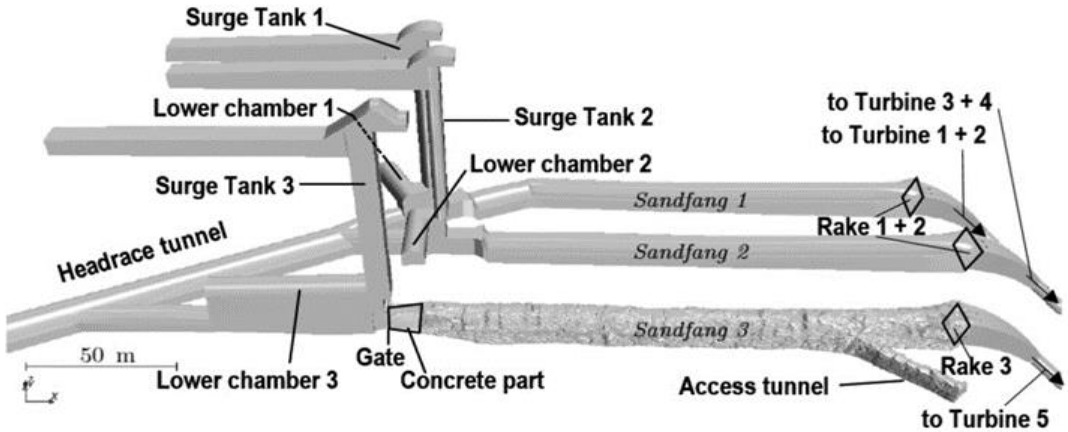

Figure 7 Overview of the unlined surge tanks and sand traps (modified) (Richter et al., 2017)

Despite the construction of an additional pressure shaft, surge tank, and sand trap, the headrace system was not upgraded stating that the new surge tank could handle resonance issues caused by the unfavorable start-up and shutdown of turbines. However, in 2000, an unfavorable operation led to an incident where free surface flow entered Sand Trap 3. This resulted in sediment flushing, which potentially damaged two turbines, caused operational downtime, and led to economic losses due to repair costs and reduced power generation revenue. Unlike Sand Traps 1 and 2, Sand Trap 3, constructed in 1988, was not subjected to any model testing at the time.

As shown in the figure below, Sand Trap 3 is situated between the gate and the trash rack. It is 191 meters long with a cross-sectional area of 119 square meters. The maximum turbine discharge is 80 cubic meters per second, resulting in an average velocity of approximately 0.67 meters per second.

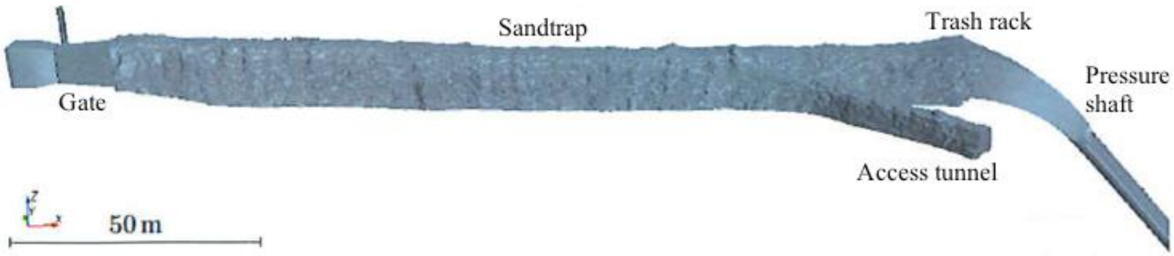

Figure 8 Sand trap 3, Tonstad hydropower plants (Steinkjer, 2018)

4.2 Scaling

Testing new designs and concepts at a full-scale prototype such as spillways, dams or canals can be significantly expensive and riskier. There will be catastrophic consequences in case of failures. To tackle this, scale models can be used which are replications of real phenomena but in a reduced size. They are comparatively less expensive and safer to conduct experiments with. Before construction, almost every project in hydraulic engineering undergoes a model test with which we can observe and measure various aspects and consequences related to the project. Based on that we can determine the most effective design scheme for implementation.

A physical scale model can achieve complete similarity and no scale effects with its prototype by satisfying mechanical similarity which comprises the following three criteria:

Geometric similarity, Kinematic similarity, Dynamic similarity

To achieve geometric similarity, the model and prototype must have the same shape and all the model's length dimensions must be λ times less than the prototype's. The kinematic similarity implies not only the geometric similarity but also the similarity of particle motion between prototype and model. This means that the ratios of time, velocity, acceleration, and discharge are kept constant between the model and the prototype. The dynamic similarity states that in addition to geometric and kinematic similarities, the ratio of all forces in the model and prototype should be the same. Some examples of forces are inertial force, gravity force, viscous force, surface tension, elastic compression force, and Pressure force. Dynamic similarity requires that the ratios of these forces stay constant between the model and the prototype. For example, the ratio of inertial force in the prototype to the model should be the same as the ratio of gravity force in the prototype to the model, and so on. The inertial force fluid dynamics is included in several common force ratio combinations, such as:

Table 2 Dimensionless numbers with formulas (Zwart, 2009)

Symbol	Definition	Formula
Froude number	(inertial force/gravity force) $^{1/2}$	$V/(gL)^{1/2}$
Reynolds number	inertial force/viscous force	LV/v
Weber number	inertial force/surface tension force	$\rho V^2 L/\sigma$
Cauchy number	inertial force/elastic force	$\rho V^2/E$
Euler number	pressure force/inertial force	$p/\rho V^2$

Where V is the characteristic velocity, L is the characteristic length, g is gravitational acceleration, v is kinematic viscosity, ρ is fluid density, σ is surface tension, E is Young's modulus, and p is pressure. Although it has been mentioned that the ratio of forces should be constant between the prototype and model, it is not achievable frequently because of various reasons. For ex, in Froude's number, the scale ratio for gravity will always be 1 and cannot be scaled up or down. In the case of sediments, the laws of similarity do not apply for the particles having a size less than 0.20 mm because of the flocculation effect, the scale should therefore not be too small (Bishwakarma, 2015). To avoid these issues (Yalin, 1971) has suggested avoiding the scaling of sediments.

4.3 Physical model description

Several hydraulic scale models of Tonstad sand trap no.3 were constructed and tested at NTNU, Trondheim (Richter et al., 2017). A total of four models (Two models of geometric scale ratio of 1:100 and another two models of 1:200) were used in this thesis work which was constructed at NTNU laboratory. All the pictures of the model are attached in the Appendix section. A new scaling approach has been adopted in this thesis where the average velocity and sediment size of the particles were kept at a ratio of 1:1 between the prototype and the model which were based on the suggestions from (Yalin, 1971) and (Richter et al., 2021). Since the main agenda of this thesis is to test how different roughness affects the trap efficiency, various roughness has been used and the roughness of the prototype is not scaled into the model. An open channel test rig called "Mini flume" which was already present in the lab has been used to test both models. It has a length of

2.40 m, a width of 0.18 m, and a height of 0.38 m. It was equipped with a basin, adjustable weir, and three pumps. It also has a digital flow meter to monitor the flow in the flume.

Figure 9 Mini flume - Test rig on the left and digital flow meter on the right

4.4 Reason for multiple models with the same scale ratio

For clarity, the models used in this study are designated as Model 100-A and Model 100-B for a 1:100 scale ratio, and Model 200-A and Model 200-B for a 1:200 scale ratio. Models 100-A and 200-A had been previously used by a master's student, who introduced surface roughness by gluing sand particles to their walls and ceilings.

Most of these sand particles had been washed away after previous experiments. It was determined, in consultation with Adj. Ass. Prof. Kaspar (NTNU), to remove the remaining sand particles from the walls and ceilings of these models because the focus of this master's thesis was on the roughness of the invert and many sand particles had been washed away during previous experiments. The removal of sand particles left traces of glue on the surfaces which can be seen in the figure below.

Figure 10 Model 200-A before removing glued sand

Figure 11 Model 200-A after removing glued sand and gluing sandpaper on the invert

To ensure accurate experimental results, the author decided to use Models 100-A and 200-A for experiments with sandpaper roughness and recently constructed Models 100-B and 200-B, which have similar dimensions to Models A, for experiments with the original plexiglass roughness on the walls, ceiling, and invert. This method makes it easier to compare the results from plexiglass and sandpaper roughness.

Although there was an option to exclusively use Models 100-B and 200-B, for both plexiglass roughness and sandpaper roughness, it was noted that a PhD candidate was already using these models without any surface modifications. Applying and removing sandpaper frequently on these models would be impractical, time-consuming, and risk damaging the invert of the models.

To avoid such risks and to maintain the model's reusability for future experiments, the decision was made to use Models A with the glued sandpaper roughness and Models B with the original plexiglass surfaces. This approach allows us to compare the results between sandpaper roughness in Model A-100 and A-200 with the plexiglass roughness in Models B-100 and B-200.

4.5 Design of models

There were a few modifications made between the model and the prototype. The prototype has a horseshoe-shaped cross-sectional area which was modified into square-shaped geometry. Only the sand trap part has been modelled which excludes the gate, the surge tank on the upstream side of the sand trap, and the pressure shaft on the downstream side. Ribs and ramp structure have been implemented on the downstream side with four number of ribs. A point to be noted is that trap efficiency doesn't change by adding more than four ribs (Richter et al., 2021)

4.6 Model 100-A

It has a geometric scale ratio of 1:100 from the prototype. A plexiglass with a 5 mm thickness was used to construct the model. The dimensions of the model are 2000 mm length x 110 mm width x 110 mm height. The crown of the model is made demountable which helps in cleaning the model and implementing roughness in the model. Since it is two meters in length, two handles are fixed for better handling. At the downstream end is the rib and ramp structure with a total length of 262 mm. Dimensions of the ramp are 192 mm length x 110 mm width x 15 mm height with a slope of 4.5°. It is made of steel with 2 mm thick.

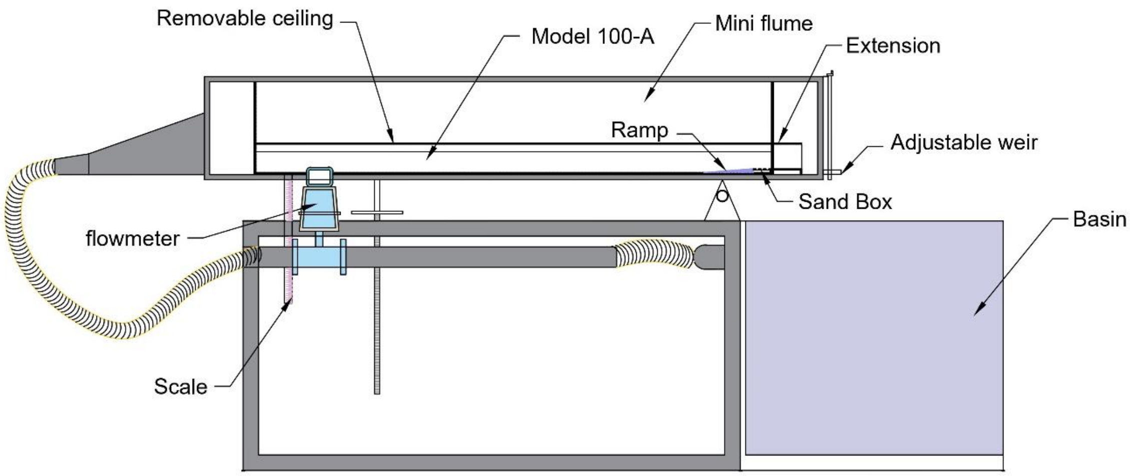

Figure 12 Hydraulic model of Tonstad sand trap no. 3 (Model 100-A) inside the mini flume

The ribs section is made of plexiglass with steel plates of 1 mm thick on the bottom and rear section to prevent the sand from spreading out of the section. It is demountable. After every test, the sand gets trapped in the ribs section which then will demounted to collect, dry, and weigh the sand. Since this section helps to collect the sand, it has been named a sandbox. The dimensions of the sandbox are 70 mm length x 110 mm width x 15 mm height with each rib separated by a spacing of 10 mm.

Figure 13 Sandbox of model 100-A with ribs

Next to the sandbox, a portable extension component was attached to reduce the turbulence of flow near the sandbox thereby preventing the escape of sand from the sandbox. Below figure represents the dimensions of the extension box.

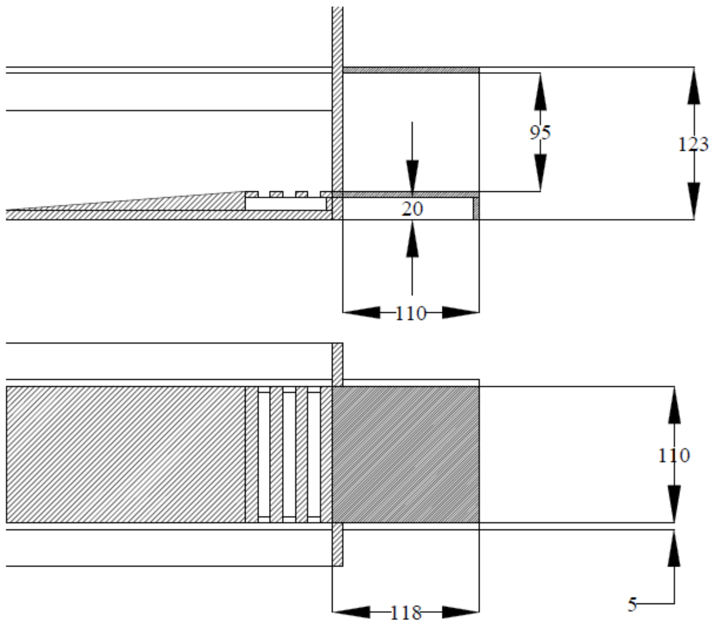

Figure 14 Extension component details from Model 100-A

At both ends of the model, acrylic plates of dimensions 8mm length x 180 mm width x 360 mm height have been attached. It will ensure sediments will pass through the model and not above the ceiling. Also, they help in achieving a pressurized flow by having water to a certain height over the ceiling. This approach offers several advantages for the construction and operation of the model test, providing high safety against breakage, a common issue with acrylic glass models (Richter et al., 2021).

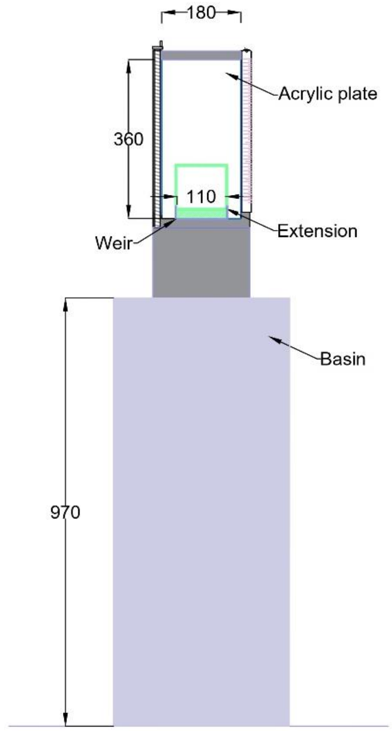

Figure 15 Cross section of Hydraulic model 100-A of Tonstad sand trap no. 3

4.7 Model 100-B

Model 100-B is exactly similar to model 100-A with fewer exceptions such as

1. Model 100-A has 4 ribs and 3 holes whereas Model 100-B has 5 ribs and 4 holes. To compare results between Model 100-A and 100-B, the 4th hole is sealed with polystyrene material in Model 100-B.
2. Model 100-B's length of the sandbox is 90 mm. The rest of the sandbox dimensions are the same as Model 100-A
3. Model 100-A has a single-piece liftable roof of 2000 mm length whereas Model 100-B has liftable roofs segregated into several compartments.
4. Model 100-A has a removable extension component near the sandbox to avoid turbulence whereas Model 100-B has a fixed continuous component.
5. Acrylic plates at both ends of the model B are removable.

4.8 Model 200-A

Model 200-A is a scaled model at a reduced geometric scale ratio of 1:200 from the prototype. Its dimensions are 1000 mm length x 55 mm width x 55 mm height which is exactly half the dimensions of Model 100-A. The design layout is almost similar to model 100-A with some exceptions.

1. A 3 mm thick plexiglass was used to make a sandbox of model 200-A. This was done to increase the storage capacity of the box.
2. Instead of steel, the ramp was made with one 8 mm piece of plexiglass and fixed to the invert.
3. Rubber strips were glued on the sides of the sandbox which prevents the sand from entering the gap between the box and walls thereby aiding in easy detachment of the sandbox from the model.
4. The extension is fixed and not removable. It is made by attaching a plexiglass plate next to the sandbox. The dimensions of the plate are 110 mm length x 55 mm width x 8 mm height.

4.9 Model 200-B

Model 200-B is exactly similar to model 200-A with fewer exceptions such as

1. Model 200-A has 4 ribs and 3 holes whereas Model 200-B has 5 ribs and 4 holes. To compare results between Model 200-A and 200-B, the 4th hole is sealed with polystyrene material in Model 200-B.
2. Model 200-B's length of the sandbox is 45 mm. The rest of the sandbox dimensions are the same as Model 200-A
3. Model 200-A has a single-piece liftable roof of 1000 mm length whereas Model 200-B has liftable roofs segregated into several compartments.
4. Acrylic plates at both ends of the model 200-B are removable.

4.10 Roughness conditions

Although sand trap no.3 of Tonstad has been taken as a prototype, the roughness is not scaled into the model as the main agenda of the thesis is to check how different roughness conditions on the invert implemented in the model impact the trap efficiency. Hence the idea was to choose a specific roughness for Model 100-A and to scale down and apply the roughness in Model 200-A and to compare the results.

4.11 Material for roughness

Sandpaper was chosen as a roughness material to impart roughness in the model. It is made of paper or cloth sheets with an abrasive material adhered to one side. It can be used to smooth out surfaces (like in painting and wood finishing), remove a layer of material (like old paint), or occasionally make the surface rougher (like in gluing preparation). Sand and glass have been replaced in the production of these products nowadays by various abrasives like silicon carbide or aluminum oxide. In order to remove material from surfaces, sandpaper comes in a variety of grit sizes. The sandpaper of grit numbers 60 and 100 from the Mirka brand was used. The sandpaper has a dimension of 2500 mm length x 115 mm width and can be carved to fit inside the models. It is made of aluminum oxide. The grit number is a rating given based on the size and number of the abrasive material embedded in the sandpaper per square inch. With smaller-sized particles, large quantities of particles can be placed per square inch of the sandpaper which also has a smoother surface. If the size is bigger, only a few particles can be placed per square inch and the surface will be rough. In general, with a higher grit number, the surface will be smoother and rougher when the grit number is lower (Leroux, 2014).

Table 3 Different grit size sandpapers and their uses (Leroux, 2014).

Grit	Common Name	Uses
30-60	Coarse	Heavy sanding and stripping roughing the surface
80-120	Medium	Smoothing the surface removing small imperfections/marks
150-180	Fine	Final sanding of the surface before finishing
220-240	Very Fine	Sanding between coats of stain or sealer

A test was conducted by (Leroux, 2014) using 3D profilometry to determine sandpaper roughness. Two different brand sandpapers (3M and Norton) of various grit sizes were tested for different height parameters.

Table 4 Height parameter measurements (Leroux, 2014)

Company	Grit	Ssk	Sku	Sq (µm)	Sp (µm)	Sv (µm)	Sz (µm)	Sa (µm)
3M	60	0.8474	3.586	83.82	549	256.7	805.8	67.09
Norton	60	0.6728	4.083	71.47	440.4	198.7	639.1	55.4
3M	100	1.099	4.135	41.05	266.5	103.6	370.1	32.42
3M	120	1.099	4.187	31.18	203.6	69.59	273.2	24.41
Norton	120	1.051	5.323	27.93	208.4	83.84	292.2	21.28

Table 5 Grit ratio of average roughness comparison between different sandpaper brands

Company	Grit	Sa	Grit 60 : Grit 120 ratio
3M	60	67.09	2.7
3M	120	24.41	
Norton	60	55.4	2.6
Norton	120	21.28	

From the above table, the column Sa represents the average roughness. It can be seen that the ratio of average roughness (Grit 60 : Grit 120) is almost the same between sandpapers of 3M and Norton, which are two different companies. So, sandpapers will have nearly the same ratio of their surface roughness irrespective of which companies they are from. Considering this fact, the Mirka sandpaper used in the experiments has assumed the average surface roughness of 3M sandpaper as mentioned in the table below.

Table 6 Average roughness (Sa) in the models

		Average Roughness - Sa (µm)	Average Roughness - Sa (mm)
Model	Scale ratio	Invert	Invert
100-A	100	67.09	0.067
200-A	200	32.42	0.032

Table 7 Height parameters developed from ISO 4287 and JIS B0601(Keyence corporation of America, 2012)

Height Parameter	Description	Notes
Sq	Root mean square height	This parameter corresponds to the standard deviation of distance from the mean plane. It is equivalent to the standard deviation of heights.
Ssk	Skewness	This parameter represents the symmetry of height distribution.
Sku	Kurtosis	This parameter represents the kurtosis of height distribution.
Sp	Maximum peak height	This parameter represents the maximum value of height from the mean plane of the surface.
Sv	Maximum pit height	This is the absolute minimum value of height from the mean plane of the surface.

Sz	Maximum height	This parameter represents the distance between the highest point and the lowest point on the surface.
Sa	Arithmetical mean height	This is the arithmetic mean of the absolute value of the height from the mean plane of the surface.

The height parameter Sa represents the arithmetical mean height or average roughness. It is the same as absolute roughness ε (mm). With Reynolds number Re, cross section width D (mm), and absolute roughness ε (mm), the friction factor and head loss of the system can be determined using the moody diagram.

4.12 Roughness implementation in the model

From the below table, sandpaper with absolute roughness of 0.067 mm and 0.032 mm has been chosen for scaled models 1:100 and 1:200 respectively. The roughness was implemented only on the invert. The walls and ceiling were left with plexiglass roughness as it has a minor effect on sediment trapping compared to invert roughness (Richter et al., 2021). It has an absolute roughness ratio of 1: 2.09 between the two models.

Table 8 Absolute roughness used in the models.

Absolute roughness ε (mm)			
Model	Scale ratio	Invert	Walls & ceiling
100-A	100	0.067	0.0015
200-A	200	0.032	0.0015

Implementation of roughness in the model has been described in the below steps.

Step 1: The first step is to clean the model with water to remove debris. For that, the model was placed inside the flume and flushed with water. After that model was removed carefully from the flume, all the water remains were wiped using a clean cloth.

Step 2: After being certain that the model is dry, double-sided tapes from the brand "super tape" were used. The dimensions of the tape are 12 mm width x 2500 mm length. The tapes were placed as close as possible in the models and small gaps between the tapes were filled with removable water sealant clay.

Step 3: After placing the tapes in the model, the top cover of the tape is removed, and super glue is applied over the tapes for total length to enhance adhesion.

Step 4: Post that the sandpaper carved according to the model invert dimension is placed carefully over the invert of the model. Pressure is applied by hand throughout the length of the sandpaper to ensure that the sandpaper is completely glued to the invert without any air gaps. This setup is left for 24 hours as the glue might take time to set.

Step 5: After 24 hours, the model implemented with sandpaper roughness is ready for experiments.

Below pictures illustrates the steps mentioned above.

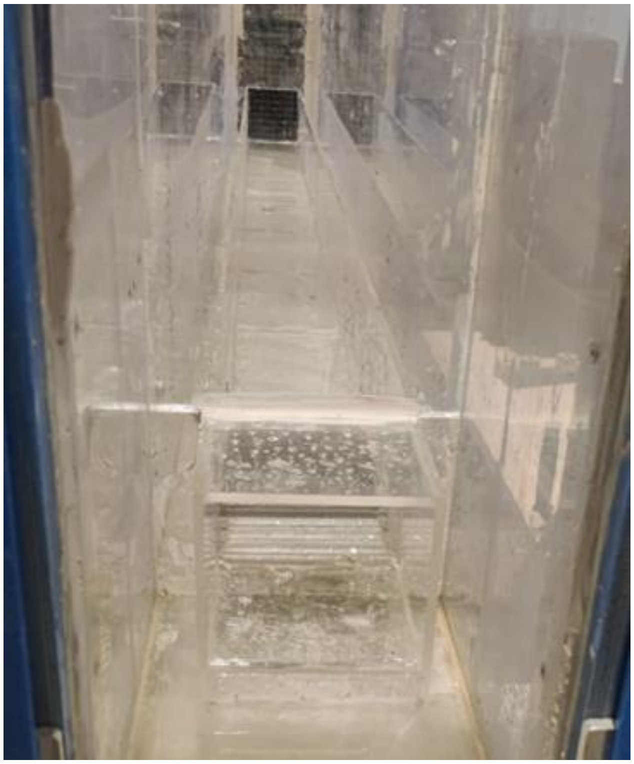

Figure 16 Cleaning the model with water

Figure 17 Double-sided tapes placed on the invert

Figure 18 Water sealant clay between gaps of tapes

Figure 19 Application of super glue over double-sided tapes

Figure 20 Placement of sandpaper over the invert

4.13 Experimental plan

The plan was to conduct experiments on four models (100-A, 100-B, 200-A, and 200-B) with two different scale ratios. Each model was tested at three different slopes with specific roughness on the invert, and each test was repeated three times for sensitivity analysis. The difference slopes in the model can be seen in the below figures.

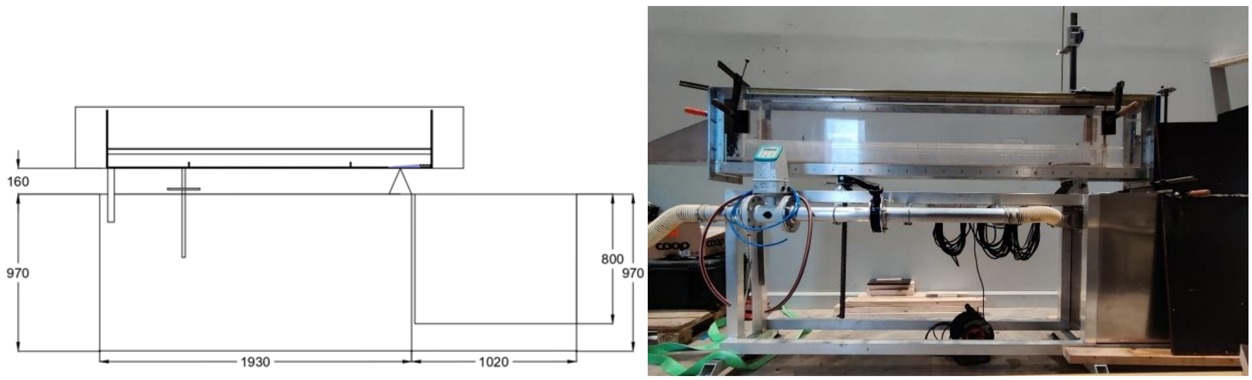

Figure 21 Model with parallel slope

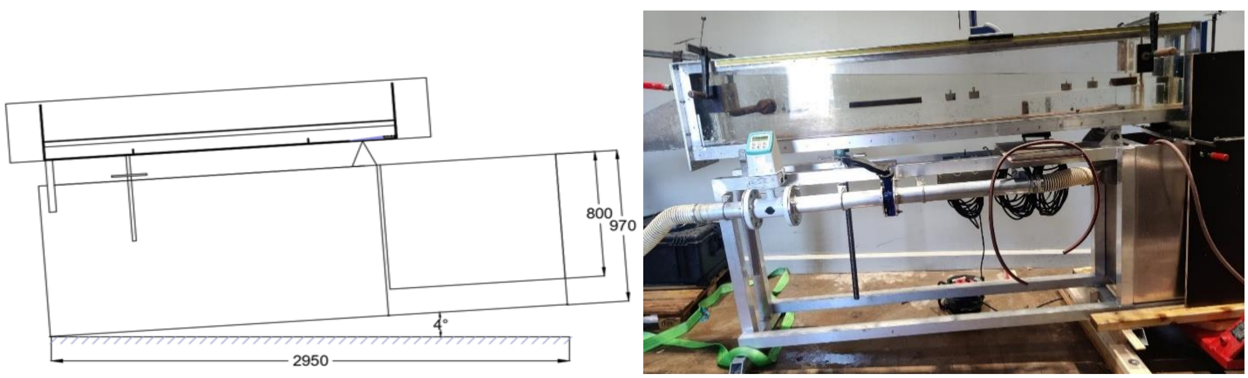

Figure 22 Model with the slope of 4° inclination

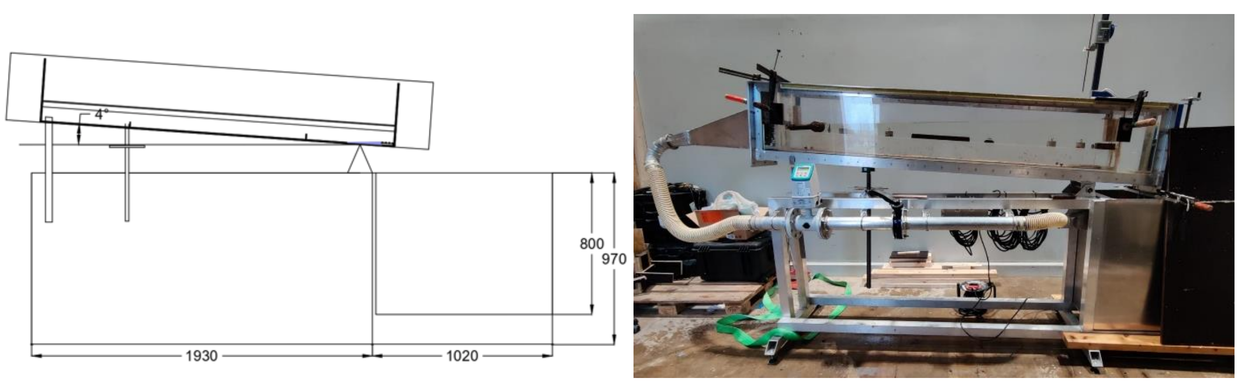

Figure 23 Model with the slope of 4° declination

A total of 36 numbers of tests were conducted. A detailed experimental plan is provided in the below table.

Table 9 Detailed experimental plan.

Experimental Plan								
Model	Scale ratio	Roughness condition	Absolute roughness over invert (mm)	Slope	Tests			Average
					1	2	3	
100-B	"1:100"	Plexiglass Roughness	0.0015	Parallel				
100-B	"1:100"	Plexiglass Roughness	0.0015	Inclined 4°				
100-B	"1:100"	Plexiglass Roughness	0.0015	Declined 4°				
100-A	"1:100"	60 Grit Sand paper	0.067	Parallel				
100-A	"1:100"	60 Grit Sand paper	0.067	Inclined 4°				
100-A	"1:100"	60 Grit Sand paper	0.067	Declined 4°				
200-B	"1:200"	Plexiglass Roughness	0.0015	Parallel				
200-B	"1:200"	Plexiglass Roughness	0.0015	Inclined 4°				
200-B	"1:200"	Plexiglass Roughness	0.0015	Declined 4°				
200-A	"1:200"	100 Grit Sand paper	0.032	Parallel				
200-A	"1:200"	100 Grit Sand paper	0.032	Inclined 4°				
200-A	"1:200"	100 Grit Sand paper	0.032	Declined 4°				

As per the 1:1 scaling approach, the velocity and sediment size of the model and prototype were kept the same. The velocity was 0.67 m/s resulting in a discharge of 8 l/s in models 100-A and 100-B and 2 l/s in models 200-A and 200-B. Sediment samples collected from Tonstad powerplant sand trap no.3 was used in the experiments.

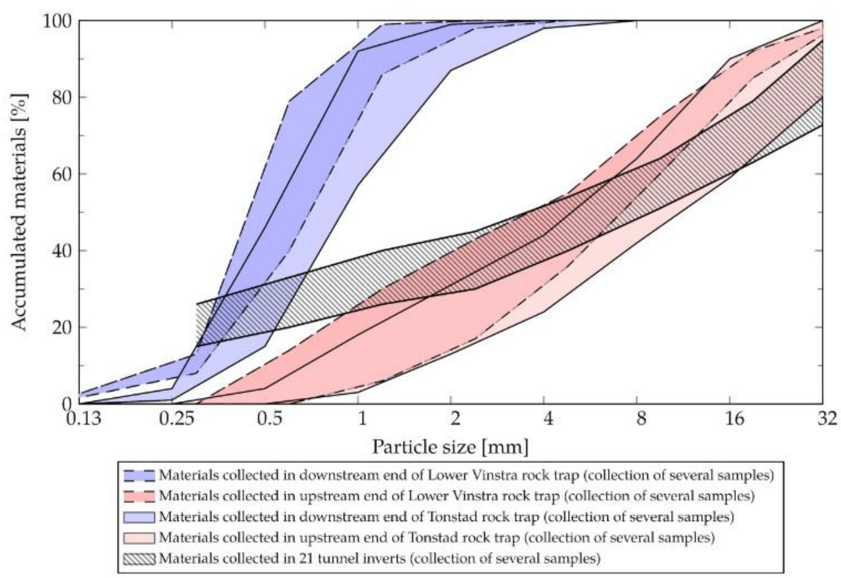

Figure 24 Particle size distribution curve of rock trap and tunnel invert of various powerplants (Havrevoll et al., 2021)

The particle size distribution curve in the above figure shows that the large-size particles (up to 32 mm) get trapped at the upstream side of the Tonstad powerplant sand trap no. 3 while small particles trapped on the downstream side of the sand trap ranges from 0.25 mm to 2mm. The major concern for turbine health is the particles found in the downstream end as they have travelled throughout the sand trap length, there are chances that these particles might escape the sand trap which might cause turbine damage. It is also noted that particles larger than 0.5 mm can cause severe damage to the turbine (Neopane et al., 2011). Hence it was decided to choose particle sizes ranging from 0.5 mm to 2 mm to use in the experiments of both the models as a 1:1 scale ratio and to check whether the sand trap can trap these sediments. The sand collected from the Tonstad sand trap was sieved using a sieve machine at the NTNU laboratory. The particles passed through a 2mm sieve and retained in a 0.5mm sieve were taken for the experiments. The density of the sand collected from Tonstad is 2650 kg/m3 and its dry density without void is 1600 kg/m3. The volume of sand input in each model was around 74% of their sandbox volume. With these data, the weight of the sand input is calculated and measured using a weighing scale with 0.01 mm precision.

The total weight 75.68 gms and 6.97 gms has been taken for models with scale ratios 1:100 and 1:200. The weighed sand is then split into small glass containers of five numbers and injected inside the model using a funnel. This is done to maintain continuous sediment supply into the model mimicking prototype scenario.

The details of sand injections and time steps can be seen in the below table.

Table 10 Sand injection and time step details

Model	Cups used	Time step (Sec)	Total time (mins)	Total Sand in (%)	Total Sand in (gms)
100-A	5	3	10	74% of Sand trap volume	75.68
100-B	5	3	10	74% of Sand trap volume	75.68
200-A	5	1.5	10	74% of Sand trap volume	6.97
200-B	5	1.5	10	74% of Sand trap volume	6.97

Figure 25 Weighing scale used for measurements

Figure 26 Glass containers used for sand injection

The test starts by switching on the pump and fixing the discharge level according to the models by adjusting the valves. Once the test starts, it takes around 12 sec and 6 sec to inject the sand into the models of 1:100 and 1:200 scale ratio. The sediments reach the sand trap within 45 sec in both models. The pump is switched off after completing the test. The flume is dewatered by lowering the weir and the ceiling lids are lifted. After that, the sandbox is carefully dismounted, and the sand is transferred to a clean vessel and kept inside the oven for 30 minutes. Once the sand is dry, the measurements are taken using the weighing scale. Based on the data obtained, we can determine the amount of sand escaped using the below formula,

$$q_{s,e} = q_{s,i} - q_{s,trapped} \tag{4.1}$$

Based on the above values, we can determine the trap efficiency. After each test, the model inside the flume is pumped with water to remove any sediment that remains in the basin. Then the basin is cleaned before starting the next experiment.

5. Results and discussion

A total of 36 tests have been conducted. The results of the tests can be seen below.

Table 11 Overall experimental results

Experimental Plan								
Model	Scale ratio	Roughness condition	Absolute roughness over invert (mm)	Slope	Tests			Average
					1	2	3	
100-B	"1:100"	Plexiglass Roughness	0.0015	Parallel	70.4 %	73.7 %	74.1 %	72.7 %
100-B	"1:100"	Plexiglass Roughness	0.0015	Inclined 4°	68.6 %	70.9 %	71.5 %	70.3 %
100-B	"1:100"	Plexiglass Roughness	0.0015	Declined 4°	75.3 %	76.9 %	76.6 %	76.2 %
100-A	"1:100"	60 Grit Sand paper	0.067	Parallel	70.0 %	71.8 %	70.4 %	70.7 %
100-A	"1:100"	60 Grit Sand paper	0.067	Inclined 4°	67.9 %	70.1 %	65.9 %	68.0 %
100-A	"1:100"	60 Grit Sand paper	0.067	Declined 4°	66.8 %	65.6 %	68.0 %	66.8 %
200-B	"1:200"	Plexiglass Roughness	0.0015	Parallel	19.7 %	19.2 %	17.6 %	18.8 %
200-B	"1:200"	Plexiglass Roughness	0.0015	Inclined 4°	25.0 %	19.5 %	21.1 %	21.9 %
200-B	"1:200"	Plexiglass Roughness	0.0015	Declined 4°	17.2 %	14.6 %	15.8 %	15.9 %
200-A	"1:200"	100 Grit Sand paper	0.032	Parallel	22.5 %	18.9 %	20.5 %	20.7 %
200-A	"1:200"	100 Grit Sand paper	0.032	Inclined 4°	21.7 %	19.4 %	22.4 %	21.1 %
200-A	"1:200"	100 Grit Sand paper	0.032	Declined 4°	17.8 %	20.7 %	19.8 %	19.4 %

5.1 Results based on scale factors

From the below figure, it is evident that models with a 1:100 scale ratio have higher trap efficiency compared to models with a 1:200 scale ratio. In particular, model 100-B with a roughness of 0.0015 mm (Plexiglass) shows the highest mean trap efficiency of 73.1% whereas model 200-B with the same roughness condition only has a mean trap efficiency of 18.9%. This could be majorly due to the fact of using 1:1 scaling of sediment size where the larger sediments are at a size of 2 mm encounter a spacing of 5 mm between the ribs in 1:200 models. The larger particles might have flowed collectively and may not fit into the smaller gaps, preventing them from getting trapped. At the same time, the 1:100 model has a spacing of 10 mm providing more room for the 2 mm particles to get trapped. This implies that the scale factors do affect the effectiveness of sediment trapping and larger models will have high trap efficiency especially if we are using a 1:1 scaling approach of sediments and velocity between model and prototype

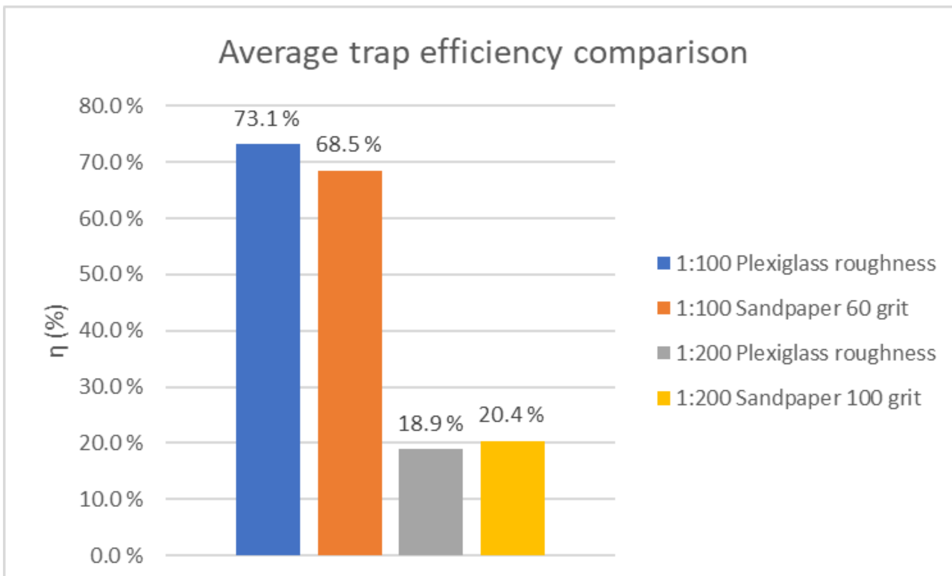

Figure 27 Comparison of models with different scale ratios and their average trap efficiencies

5.2 Results based on roughness

The effect of surface roughness on the trap efficiency was investigated by comparing models with different roughness conditions. Sandpaper (0.067 mm for 1:100 models and 0.032 mm for 1:200 models) and Plexiglass (0.0015 mm for both scale ratios) were the two roughness conditions that were examined.

In 1:100 models, Model 100-B (plexiglass - 0.0015 mm) had a mean trap efficiency of 73.1%, which is higher than Model 100-A (sandpaper - 0.067 mm) with a mean trap efficiency of 68.5%. The maximum trap efficiency in 1:100 scale models can be found in model 100-B (plexiglass) with a trap efficiency of 76.2% while the minimum can be found in the 100-A (sandpaper) with a trap efficiency of 66.8%. The overall roughness effect of model 1:100 can be witnessed below.

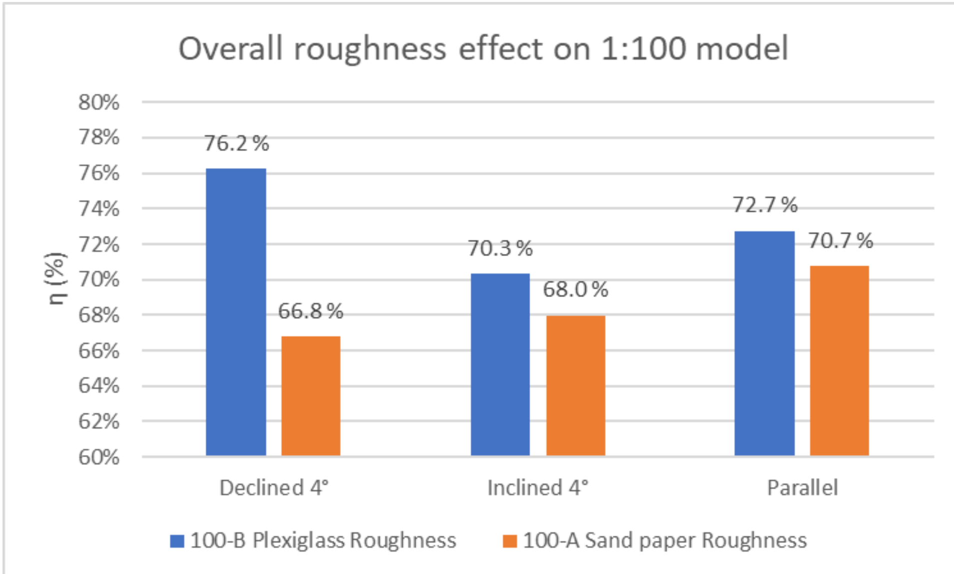

Figure 28 Overall roughness effect in 1:100 model

In 1:200 models, Model 200-B (plexiglass - 0.0015 mm) had a mean trap efficiency of 18.9 %, which is slightly lower than Model 200-A (sandpaper - 0.032 mm) with a mean trap efficiency of 20.4 %. The highest trap efficiency of 1:200 models can be found in model 200-B (plexiglass) with a trap efficiency of 21.9% while the lowest can also be found in the 200-B (plexiglass) with a trap efficiency of 15.9% at different slope conditions. The overall roughness effect of model 1:200 can be witnessed below.

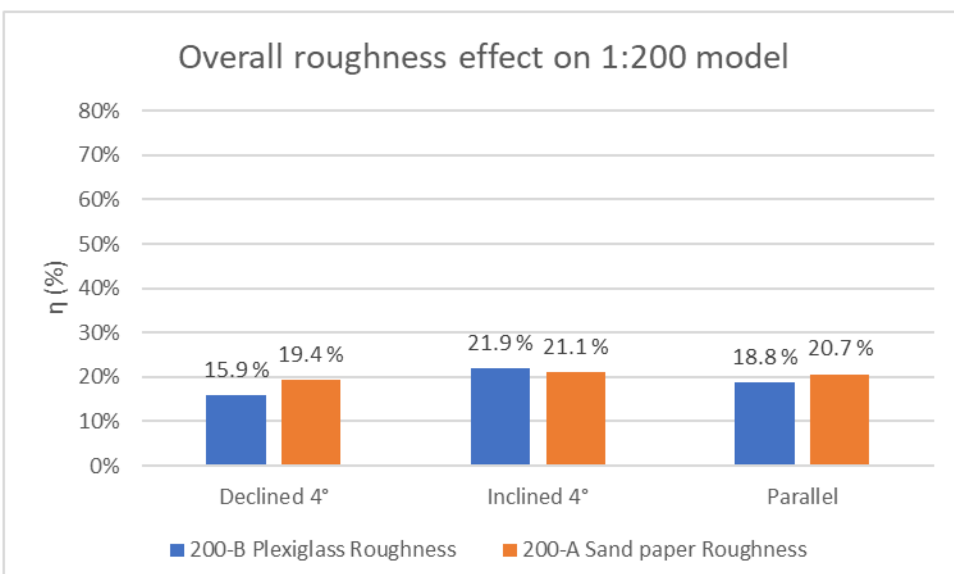

Figure 29 Overall roughness effect in 1:200 model

Comparison between 1:100 and 1:200 models on different roughness conditions for various slopes can be seen in the below charts.

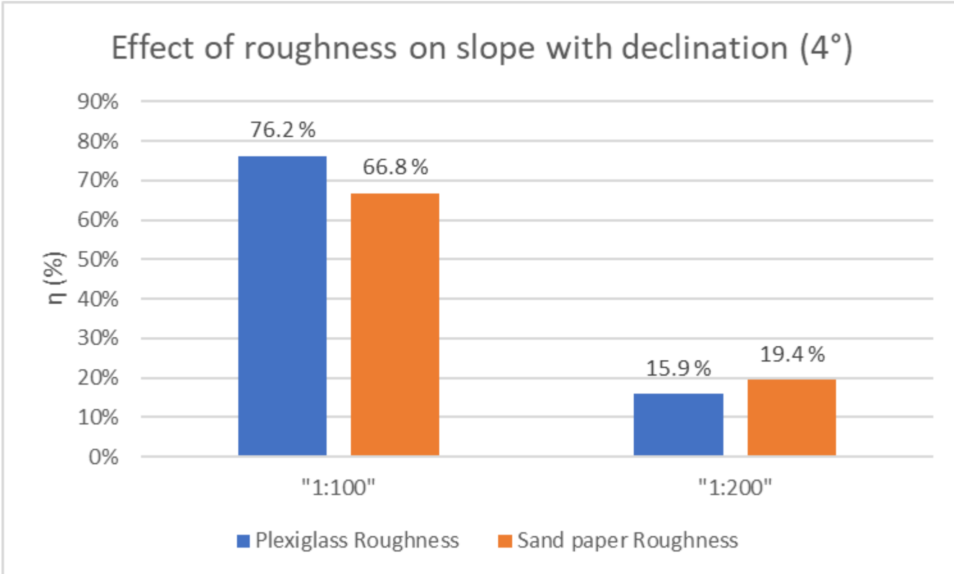

Figure 30 Effect of roughness on declined slope (4°) against trap efficiency

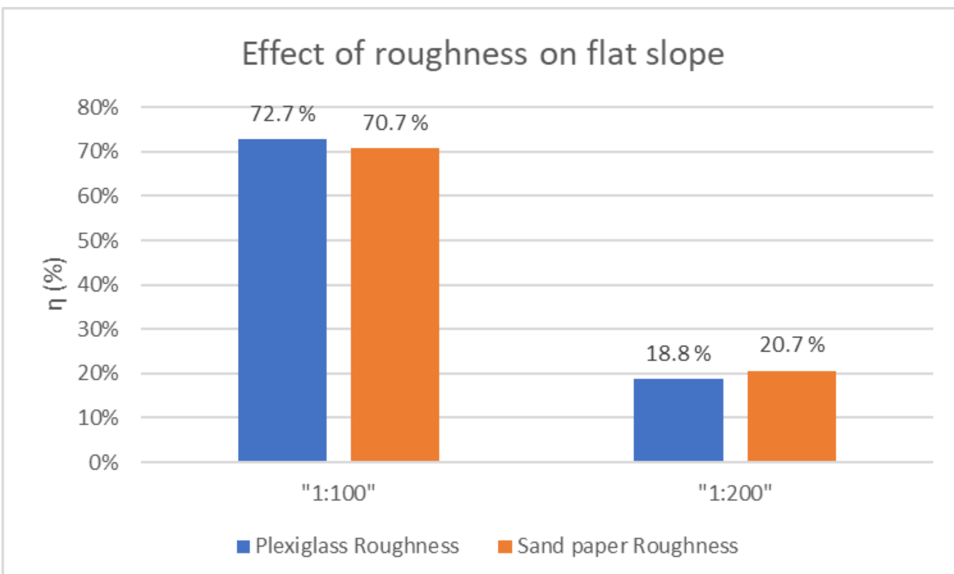

Figure 31 Effect of roughness on flat slope against trap efficiency

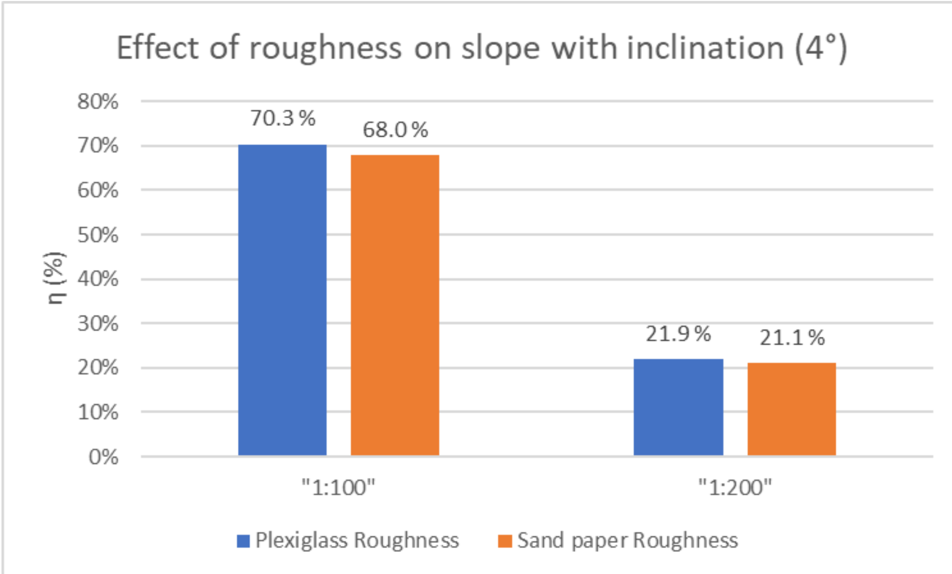

Figure 32 Effect of roughness on the inclined slope (4°) against trap efficiency

The results show that models with lower roughness (plexiglass) have higher trap efficiency in the 1:100 scale models. Specific reasons for the higher trap efficiency observed in lower roughness conditions (plexiglass) could be due to a smoother surface, which reduces the turbulence and allows more sediments to settle. However, in the 1:200 scale models, although the highest individual trap efficiency (21.9%) is found in the lower roughness (plexiglass) condition (refer to Figure 29), the average trap efficiency is slightly higher in the sandpaper roughness condition. This discrepancy could be due to the scale effects affecting sediment flow differently. The reason for these contradicting results makes it difficult to determine the best roughness conditions for having higher sand trap efficiencies in 1:200 models. Since the average trap efficiency results are not similar between the models, we cannot conclude which roughness condition is best suited for optimal trap efficiency. However, based on the highest trap efficiency values in 1:100 (76.2%) and 1:200 (21.9%) models, low roughness (plexiglass) provides favourable conditions for good trap efficiency results.

5.3 Results based on slope

The effect of slope on the trap efficiency was investigated by comparing models with different slope conditions. Models were tested with parallel, inclined (4°), and declined (4°) slopes.

In 1:100 models, with plexiglass roughness, the highest trap efficiency can be seen at declined slope conditions followed by parallel slope. The least trap efficiency can be found with inclined slope conditions. With sandpaper roughness on the invert, it's quite opposite to plexiglass roughness results. The highest trap efficiency can be found in the parallel slope while the least with the declined slope and the inclined slope being intermediate in terms of trap efficiency. Overall comparison between both the roughness conditions indicates that the highest trap efficiency (76.2%) can be found in a declined slope (4°) with plexiglass conditions whereas the lowest trap efficiency can be found in the same declined slope (4°) but with sandpaper roughness conditions on the invert. This creates an ambiguous condition to conclude the slope conditions for best trap efficiency in 1:100 models.

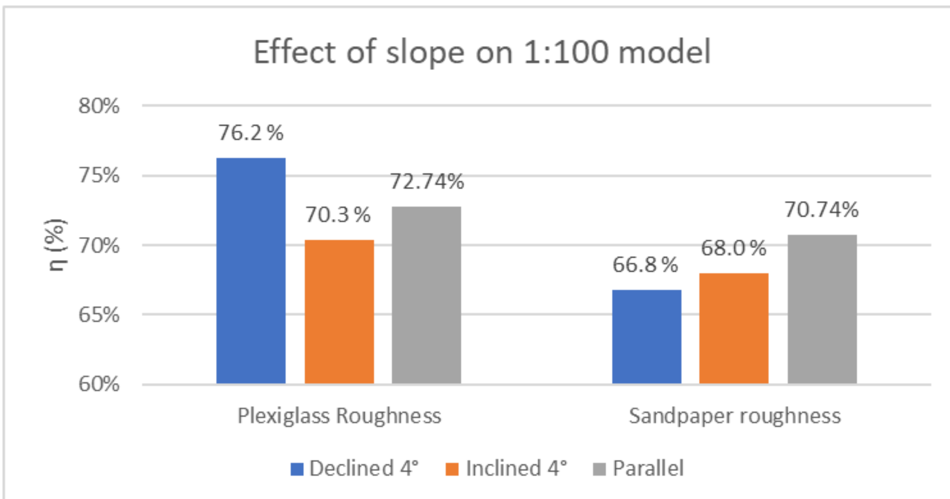

Figure 33 Effect of slope on 1:100 model

In 1:200 models, both roughness conditions exhibit the same trap efficiency pattern for different slopes. For ex, in both roughness conditions, the inclined slope has the highest trap efficiency followed by parallel and declined slope. Out of both roughness, the highest trap efficiency can be found in the inclined slope of plexiglass roughness conditions with a trapping efficiency of 21.9%.

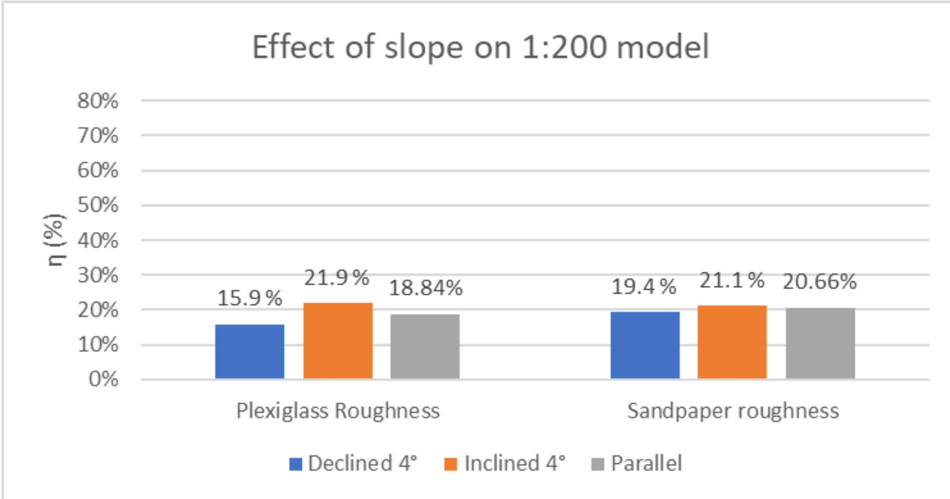

Figure 34 Figure 33 Effect of slope on 1:200 model

Meanwhile, the lowest trap efficiency can be found in a declined slope with the plexiglass roughness conditions with a trapping efficiency of 15.9%. This shows that inclined slope conditions are well-suitable for higher trap efficiency in 1:200 models.

However, the results from 1:100 and 1:200 are contradicting showing higher trap efficiency at different slope conditions. This gives uncertainty in concluding the best slope conditions.

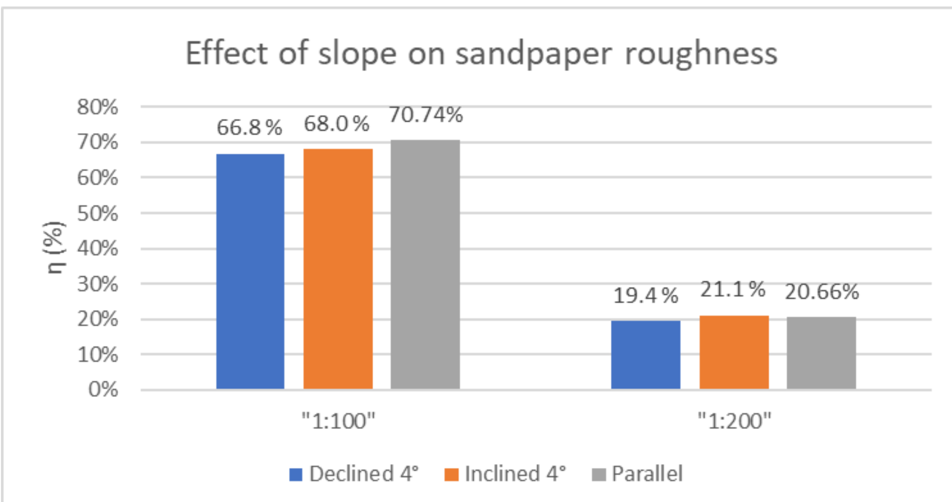

Figure 35 Slope effect comparison between two models on sandpaper roughness

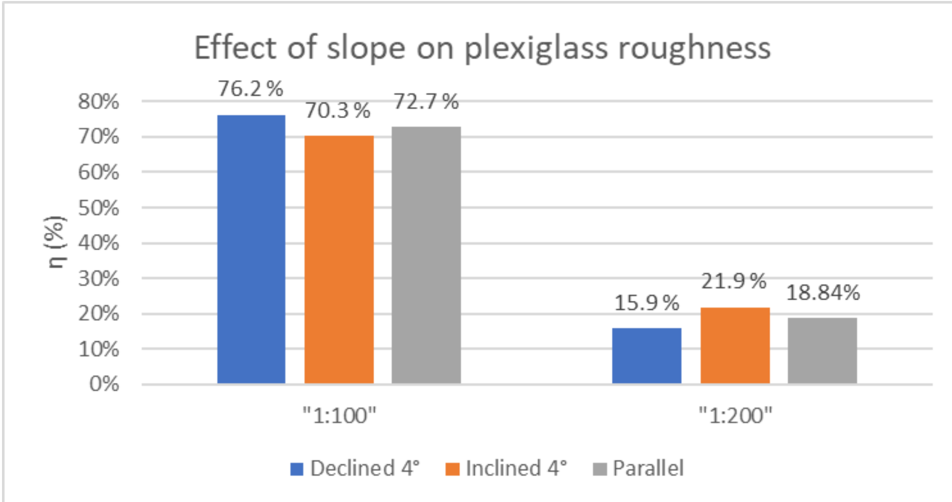

Figure 36 Slope effect comparison between two models on plexiglass roughness

The reason for different results in two different roughness conditions in the 1:100 model could be based on particle interaction on the boundary layer. Plexiglass offering less resistance might allow the particles to move smoothly whereas the sandpaper roughness might exhibit resistance over the particle's movement. This in turn might cause the particle to collide and possibly lead to suspension thus escaping the sand trap.

Based on hypothesis number one, the plexiglass roughness condition was expected to give higher efficiency because it creates less turbulence in the water flow, allowing more sediment particles to settle. On the other hand, the increased roughness from sandpaper creates more turbulence, which keeps sediment particles in suspension longer, thus reducing trap efficiency. The experimental results confirmed this, showing that models with plexiglass roughness consistently trapped more sediment compared to those with sandpaper roughness. However, this was not the case with the slope condition where the hypothesis differs significantly from test results. Different models have shown contradicting trap efficiency results concerning slope. This is definitely because of the scale effects, especially with 1:1 scaling of sediments and velocity. Hence it becomes difficult to conclude which slope contributes to the highest trap efficiency. Overall results stated that reduced roughness conditions can aid the system to achieve higher trap efficiency however best slope conditions are unclear and need further investigations.

The results are in concurrence with hypothesis number two which states that the results from 1:100 models will not be similar to 1:200 models. This is evident that the particle sizes were kept the same between both models however the gaps between the ribs of the sand trap are significantly different between both models. This gave an advantage to 1:100 models to achieve higher trap efficiency.

The second hypothesis was that the results from the 1:100 and 1:200 scale models would differ due to the unconventional scaling method where velocity and particle size were kept constant across both models. This hypothesis was also confirmed by the experimental findings. Different results were obtained because the changes in flow dynamics that occur with different geometric scales were not taken into account by having constant velocity and particle size in the models. This resulted in poor dynamic similarity, leading to scaling effects and contradicting results.

Recommendations for future work are to compare different scaling approaches with varying conditions of roughness. This might provide possible options to compare diverse results. Another recommendation is to conduct five tests for sensitivity analysis which might help us to have a solid conclusion More emphasis should be placed on determining solutions for scale effects.

6. Summary

The purpose of this study was to address sand trap issues in hydropower plants. The study concentrated on how the tunnel invert roughness and slope conditions affect the efficiency of sand traps with ribs and ramp structures in systems. Scale models, at 1:100 and 1:200 was used to test different surface roughness (Plexiglass and rough sandpaper) and slopes (parallel, inclined, and declined). The results largely vary between the two models. In the 1:100 scale models, the highest efficiency (76.2%) was achieved with a declined slope and smooth Plexiglass surface while the lowest efficiency was also found on the same slope level but with sandpaper roughness. Even though we cannot conclude which slope is suitable for higher efficiencies, it is certain that minimum roughness in the models helps them in achieving high trap efficiency. Regarding the 1:200 scale models, with plexiglass roughness, the highest trap efficiency (21.9%) was observed with an inclined slope, which is followed by a parallel (18.8%) slope, and the least trap efficiency was found in the declined slope (15.9%). The same slope rank was seen with sandpaper roughness in 1:200 models with an inclined slope having high trap efficiency (21.1%) followed by a parallel slope (20.7%) and declined slope (19.4%). Overall, the highest trap efficiency in 1:200 models between two roughness conditions can be found with plexiglass roughness (21.9%). This suggests that smoother surfaces generally lead to higher efficiency. However, determining a slope for maximum effectiveness remains uncertain due to variations in results between the two models. Further investigation is necessary to gain insights, into these distinctions.

7. References

Bishwakarma, M. B. (2015). *Settling basin designcriteria and trap efficiency computation methods*.

Havrevoll, O. H., Vereide, K., & Lia, L. (2021). Efficiency of Pressurized Rock Traps for Unlined Hydropower Tunnels. *Energies*, *14*(14), 4344. https://doi.org/10.3390/en14144344

Ivarson, M. M., Trivedi, C., & Vereide, K. (2021). Investigations of Rake and Rib Structures in Sand Traps to Prevent Sediment Transport in Hydropower Plants. *Energies*, *14*(13), 3882. https://doi.org/10.3390/en14133882

Keyence corporation of America. (2012). *Introduction to surface roughness measurement*.

Lal Maskey, D., Nepal, D., Herman, D., Gaiti, G., & Rüther, N. (2020, March 23). *3D numerical modeling of sediment handling techniques in a hydro power reservoir*. https://doi.org/10.5194/egusphere-egu2020-19713

Leod, C. M., Sawadogo, D. O., & Basson, G. (n.d.). *OPTIMIZATION OF SAND TRAP AND SETTLER DESIGNS FOR EFFICIENT DEPOSITION OF SUSPENDED SEDIMENT*.

Leroux, P. (2014). *Sandpaper Roughness Measurement Using 3D Profilometry*. Unpublished. https://doi.org/10.13140/RG.2.1.1985.4244

Neopane, H. P., Dahlhaug, O. G., & Cervantes, M. (2011). *Sediment Erosion in Hydraulic Turbines*.

Raju, K. G. R., Kothyari, U. C., Srivastav, S., & Saxena, M. (1999). Sediment Removal Efficiency of Settling Basins. *Journal of Irrigation and Drainage Engineering*, *125*(5), 308–314. https://doi.org/10.1061/(ASCE)0733-9437(1999)125:5(308)

Richter, W., Vereide, K., Mauko, G., Havrevoll, O. H., Schneider, J., & Zenz, G. (2021). Retrofitting of Pressurized Sand Traps in Hydropower Plants. *Water*, *13*(18), 2515. https://doi.org/10.3390/w13182515

Richter, W., Vereide, K., & Zenz, G. (2017). Upgrading of a Norwegian pressurized sand trap combined with an open air surge tank. *Geomechanics and Tunnelling*, *10*(5), 620–624. https://doi.org/10.1002/geot.201700027

Schwimmer, R. (2013). *Calculation of stream discharge required to move bed material*. Calculation of stream discharge required to move bed material. https://serc.carleton.edu/NAGTWorkshops/sedimentary/activities/14100.html

Simanjuntak, T., Boeriu, P., & Dano Roelvink, J. (2009). Consideration on the Sedimentation Process in a Settling Basin. *Journal of Hydrology and Hydromechanics*, *57*(1). https://doi.org/10.2478/v10098-009-0002-4

Steinkjer, S. marie. (2018). *Hydraulic Scale Modeling of Sediments for Pressurized Sand Traps*.

Vereide, K., Lia, L., Havrevoll, O. H., Richter, W., & Jakobsen, T. (2017). *Upgrading of Sand Traps in Existing Hydropower Plants*.

Yalin, M. S. (1971). *Theory of Hydraulic Models*. Macmillan Education UK. https://doi.org/10.1007/978-1-349-00245-0

8. Appendix

All the technical drawings were received from the lab technician. Technical drawings of all models with measurements in mm are given below.

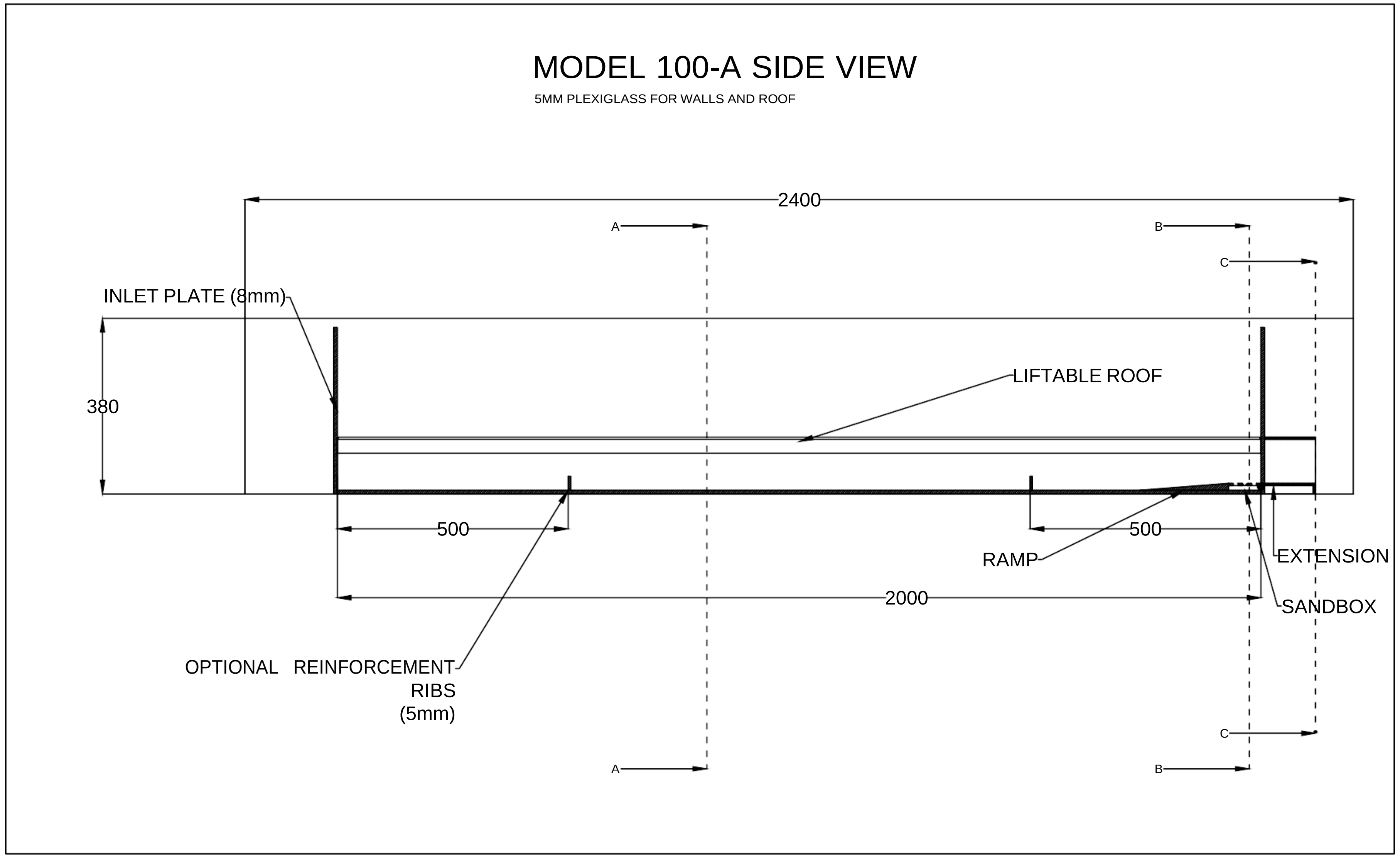

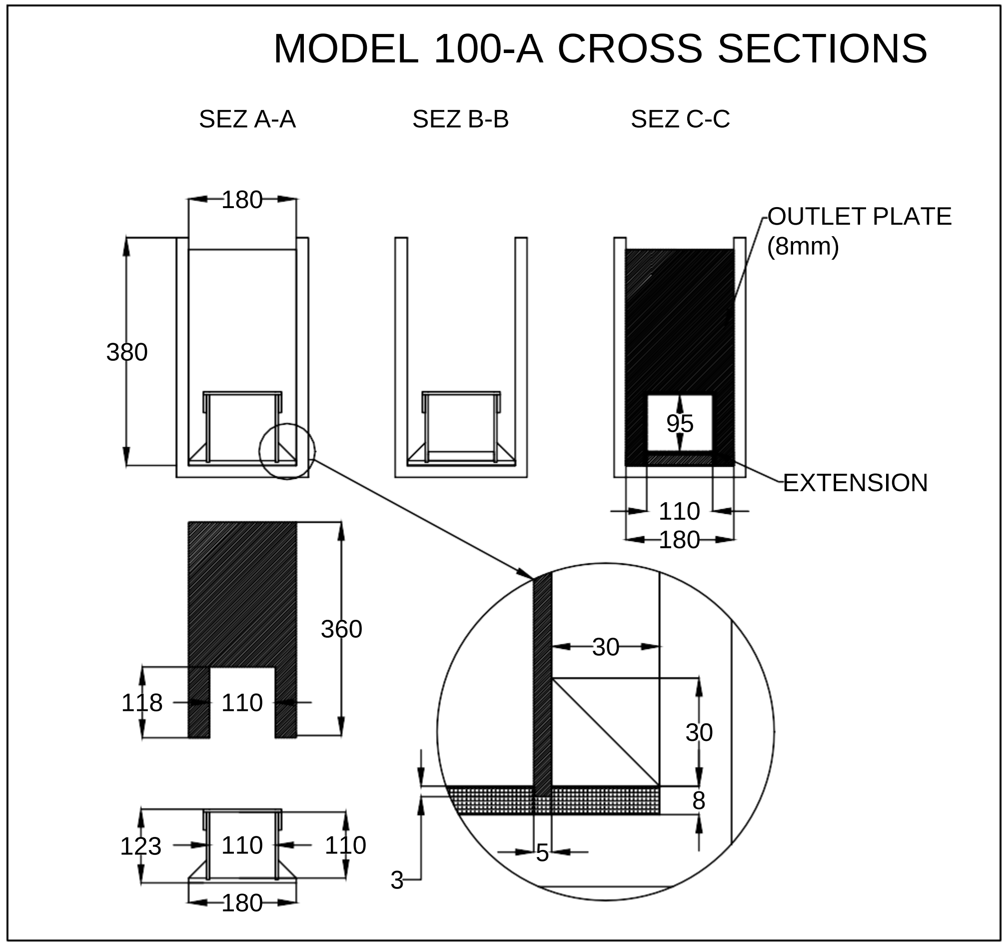

MODEL 100-A DETAILS

LIFTABLE ROOF

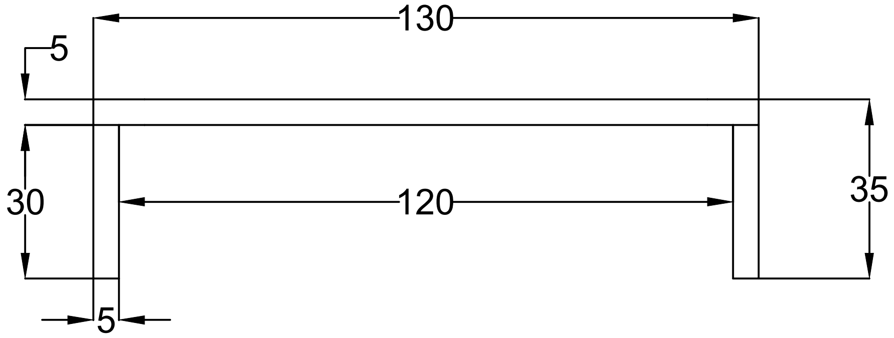

SAND BOX AND RIBS
(5MM PLEXIGLASS)

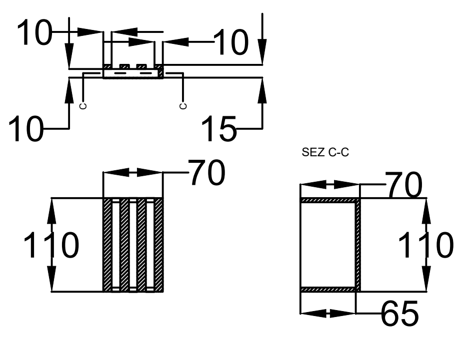

SANDTRAP

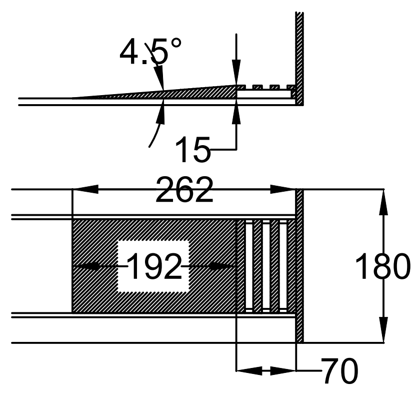

EXTENSION

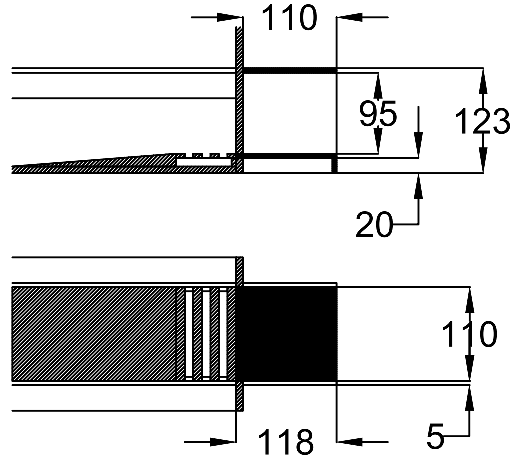

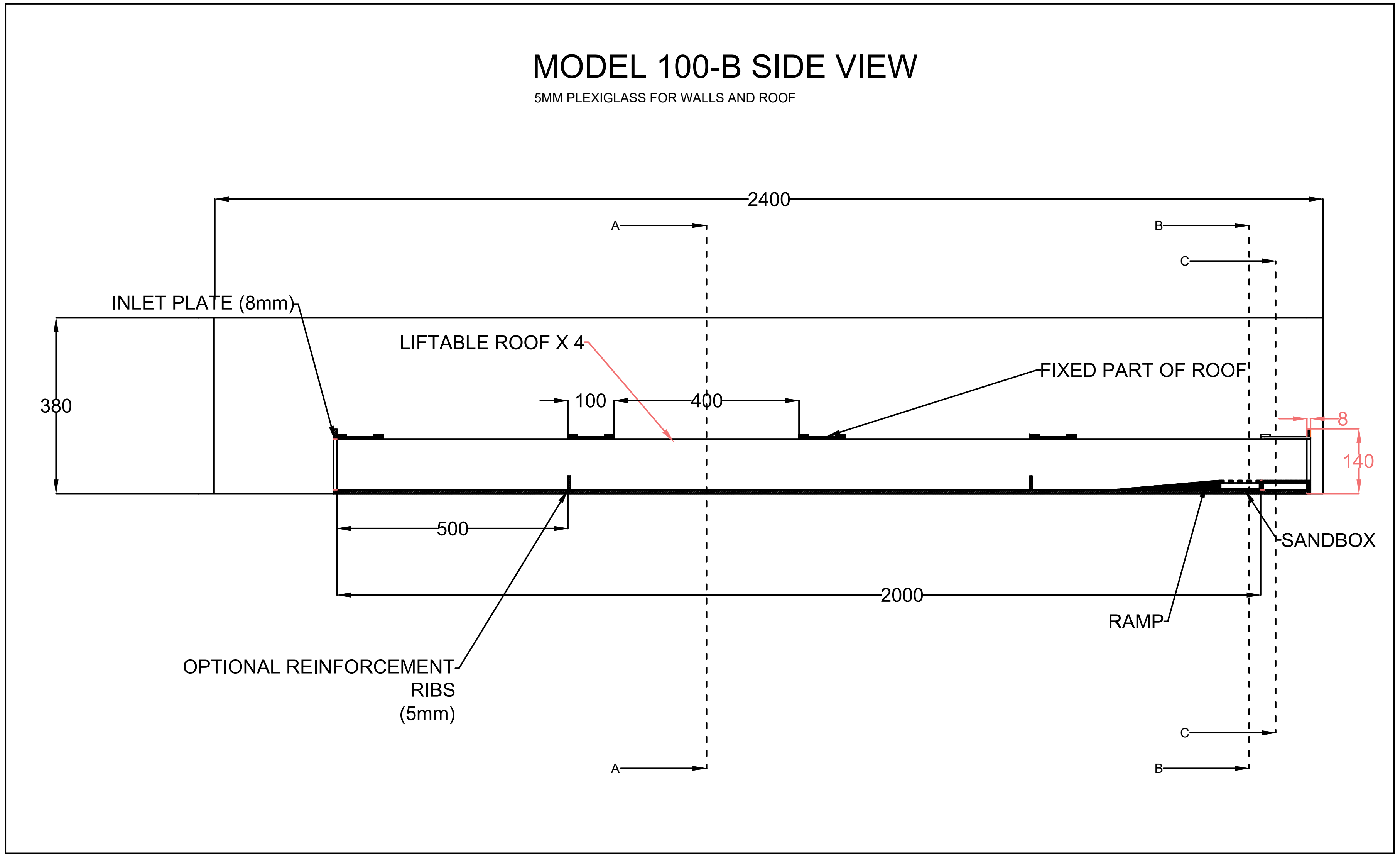
MODEL 100-B SIDE VIEW
5MM PLEXIGLASS FOR WALLS AND ROOF
2400
A
B
C
INLET PLATE (8mm)
LIFTABLE ROOF X 4
FIXED PART OF ROOF
380
100
400
8
140
500
SANDBOX
2000
RAMP
OPTIONAL REINFORCEMENT
RIBS
(5mm)

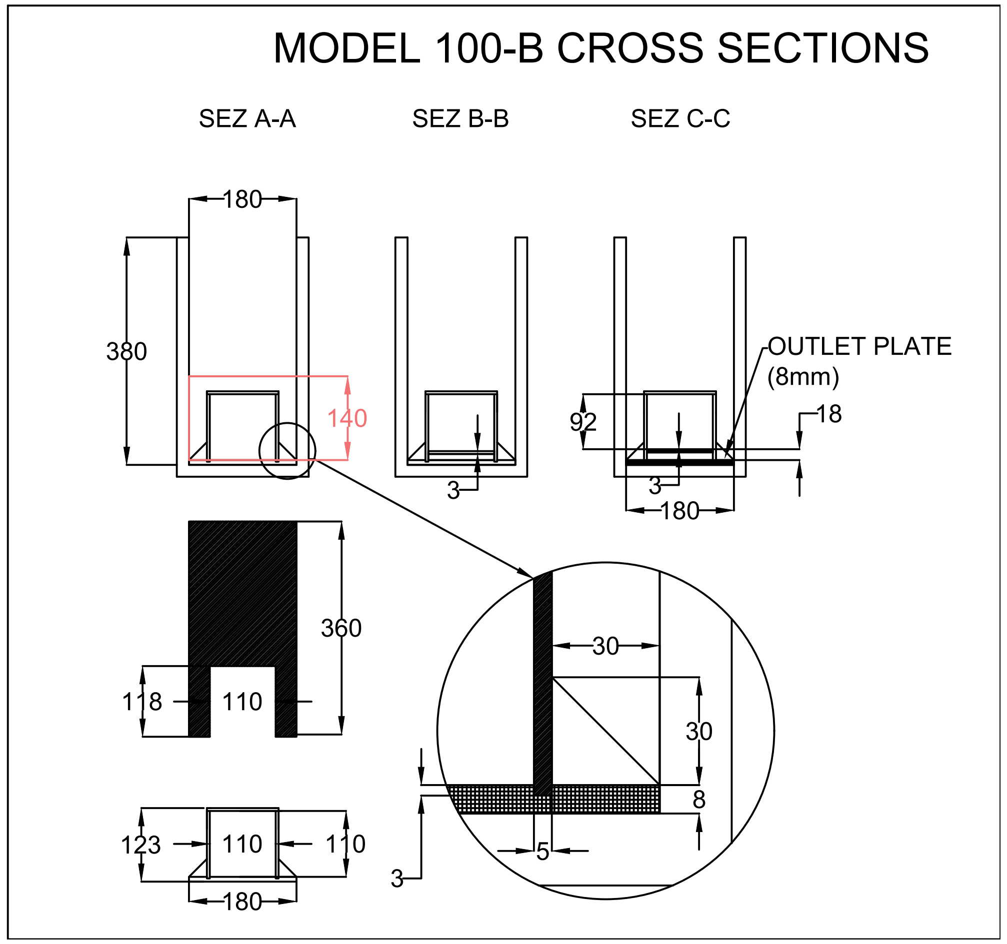
MODEL 100-B CROSS SECTIONS
SEZ A-A
SEZ B-B
SEZ C-C
180
380
140
OUTLET PLATE
(8mm)
92
18
3
180
360
118
110
30
30
8
123
110
110
180
5
3

MODEL 100-B DETAILS

LIFTABLE ROOF X 4

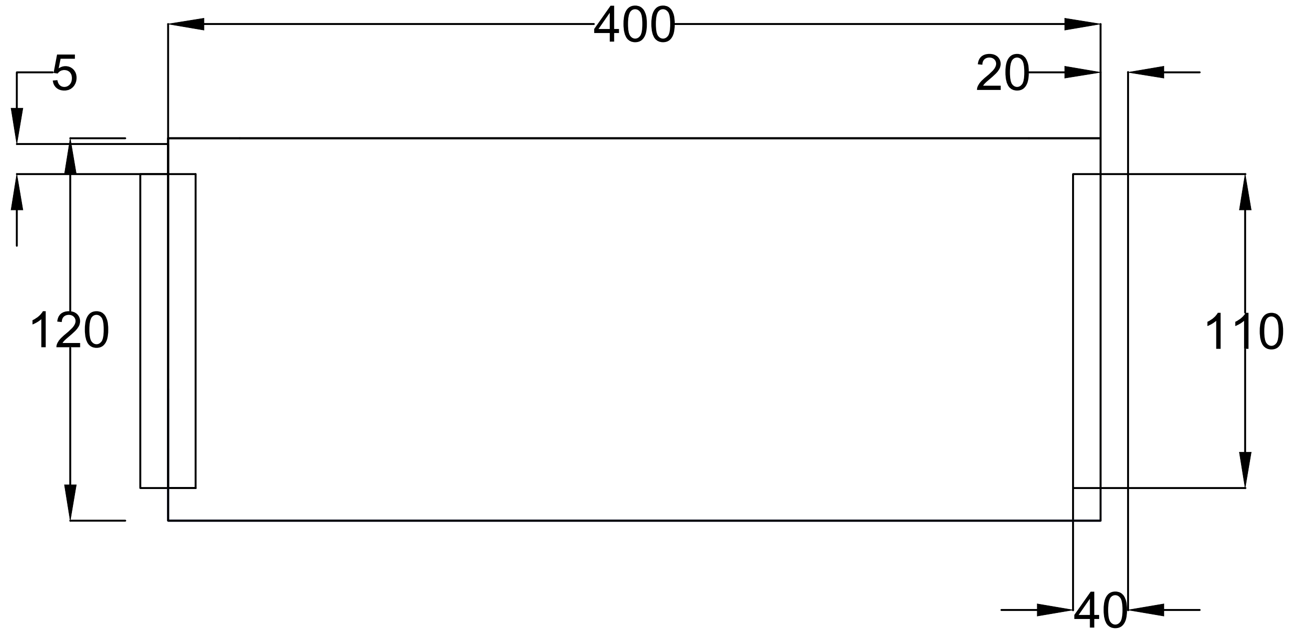

SAND BOX AND RIBS
(5MM PLEXIGLASS)

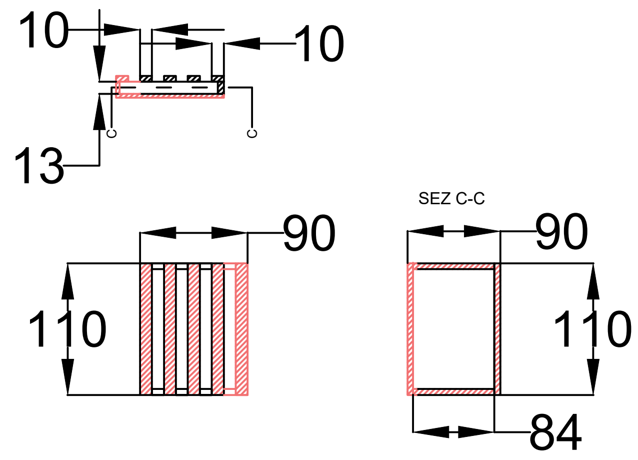

SANDTRAP

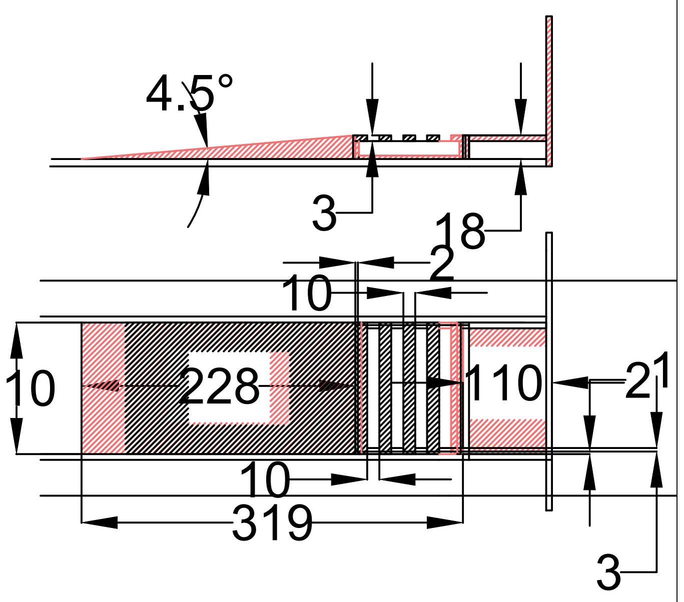

MODEL 200-A SIDE VIEW

5 MM PLEXIGLASS FOR WALLS AND ROOF

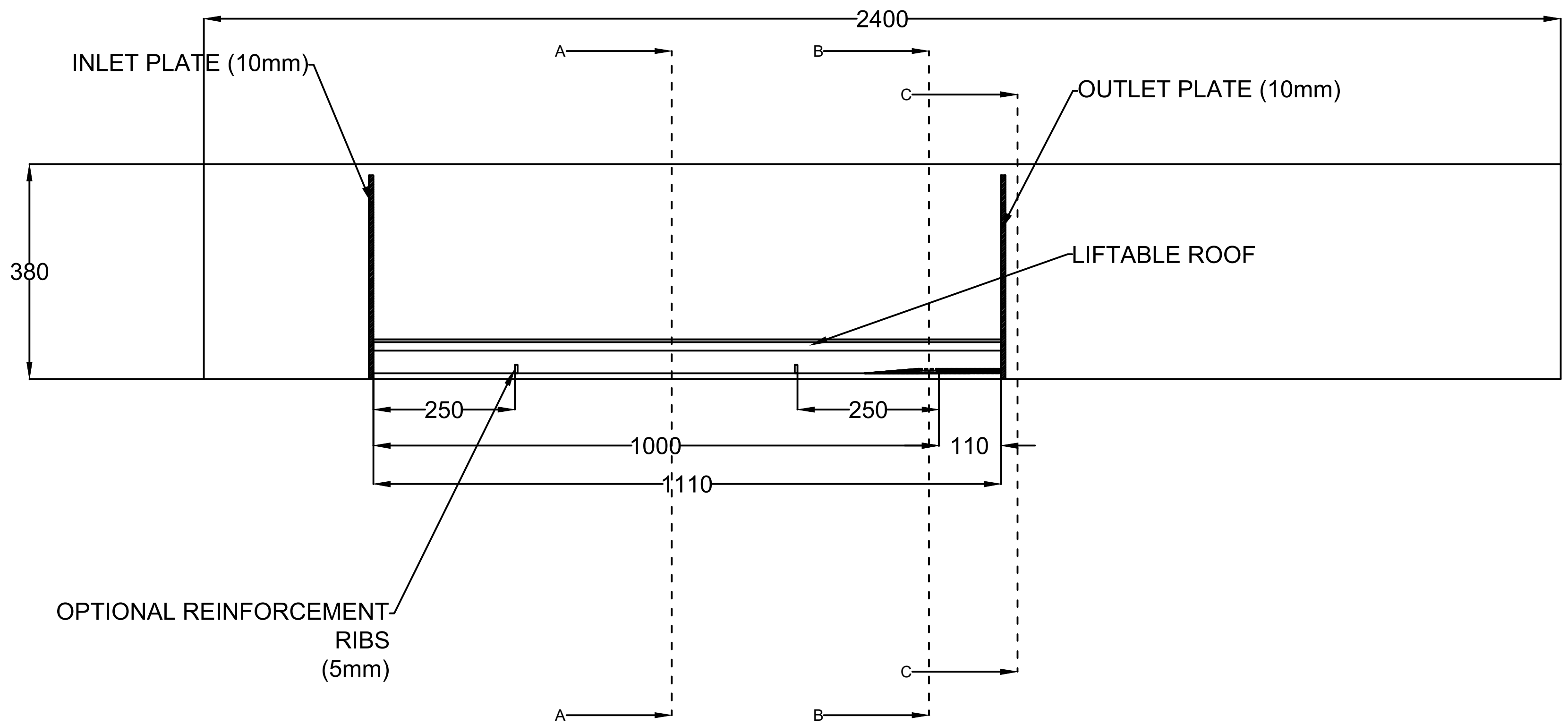

MODEL 200-A CROSS SECTIONS

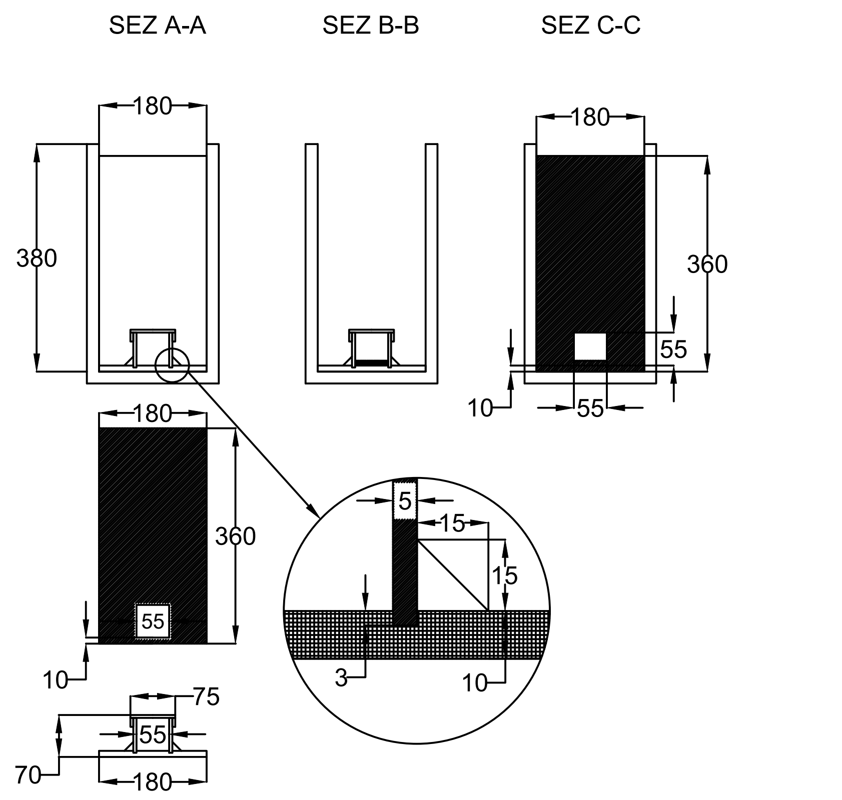

MODEL 200-A DETAILS

LIFTABLE ROOF

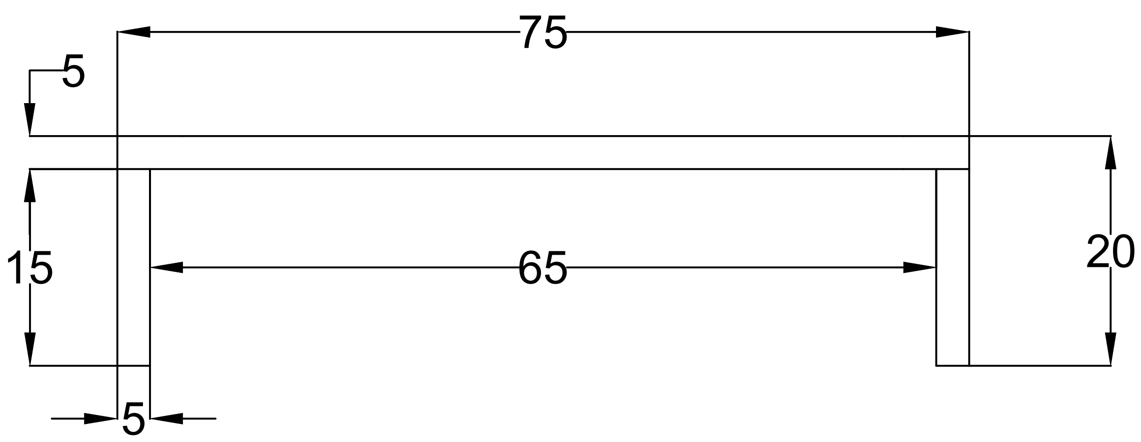

SAND BOX AND RIBS
(3 MM PLEXIGLASS)

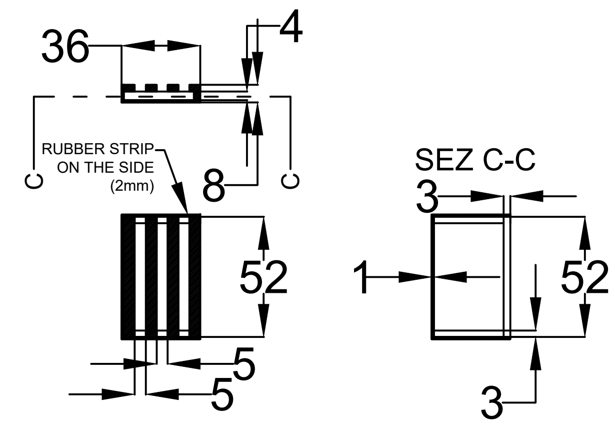

SANDTRAP

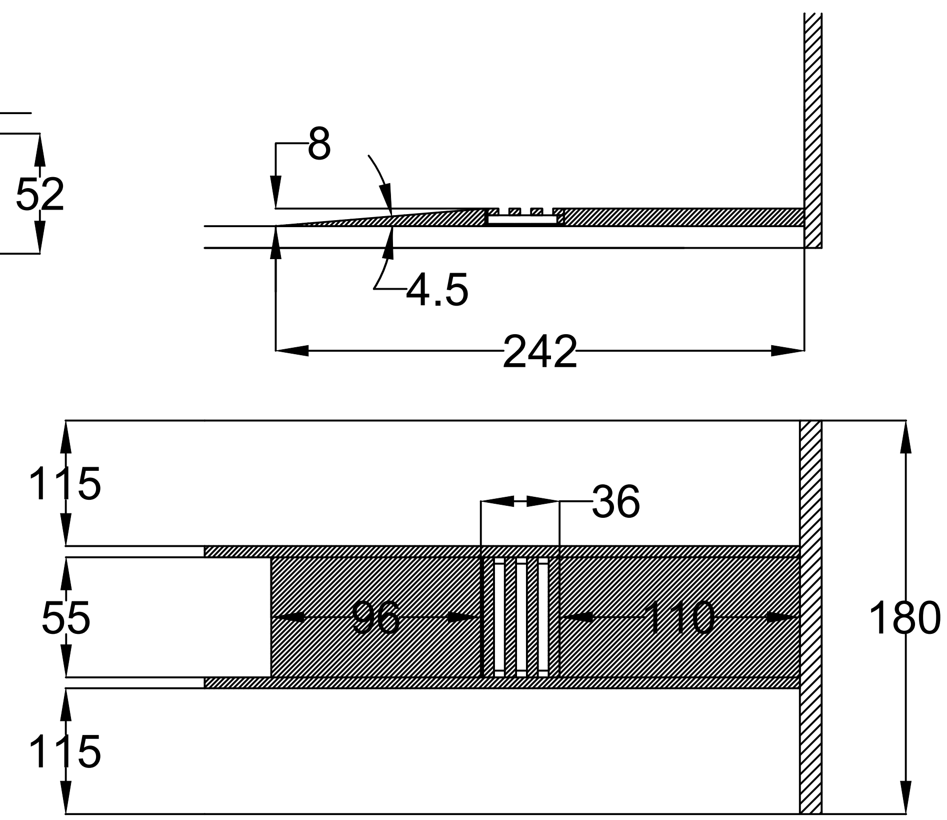

MODEL 200-B SIDE VIEW

5 MM PLEXIGLASS FOR WALLS AND ROOF

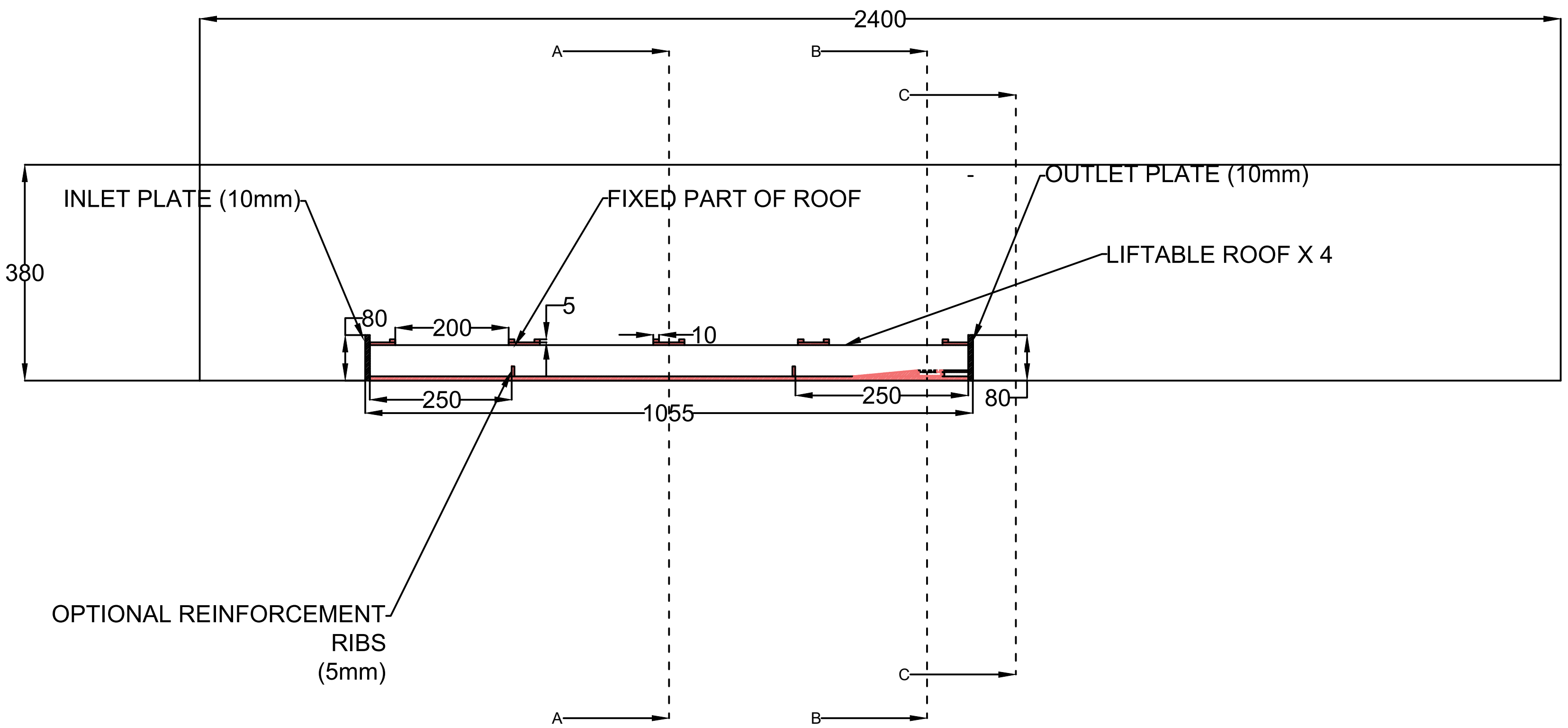

MODEL 200-B CROSS SECTIONS

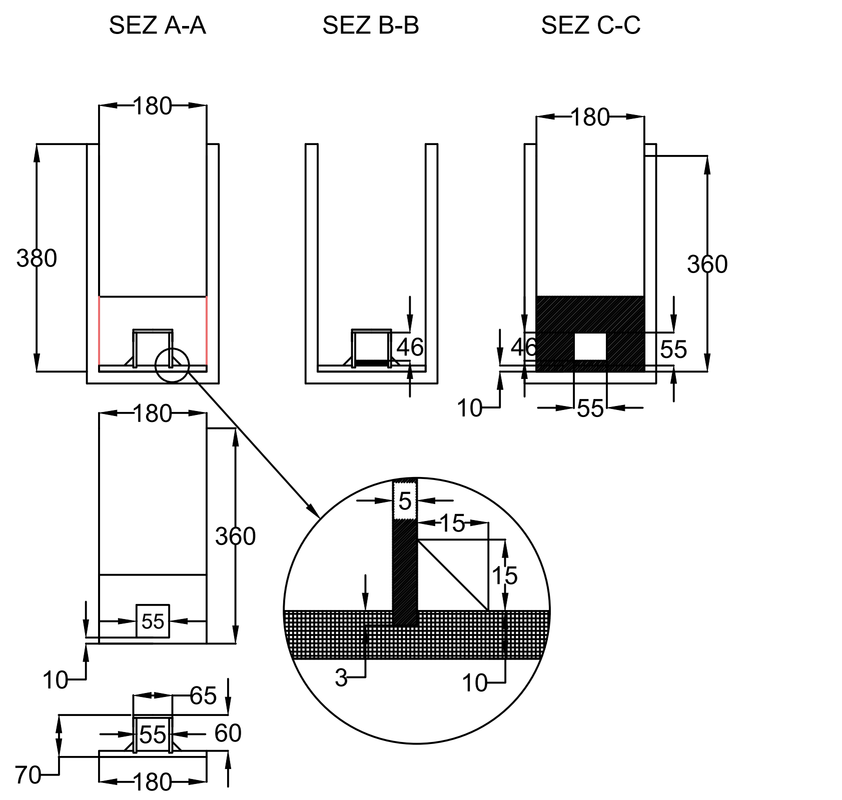

MODEL 200-B DETAILS

LIFTABLE ROOF x 4

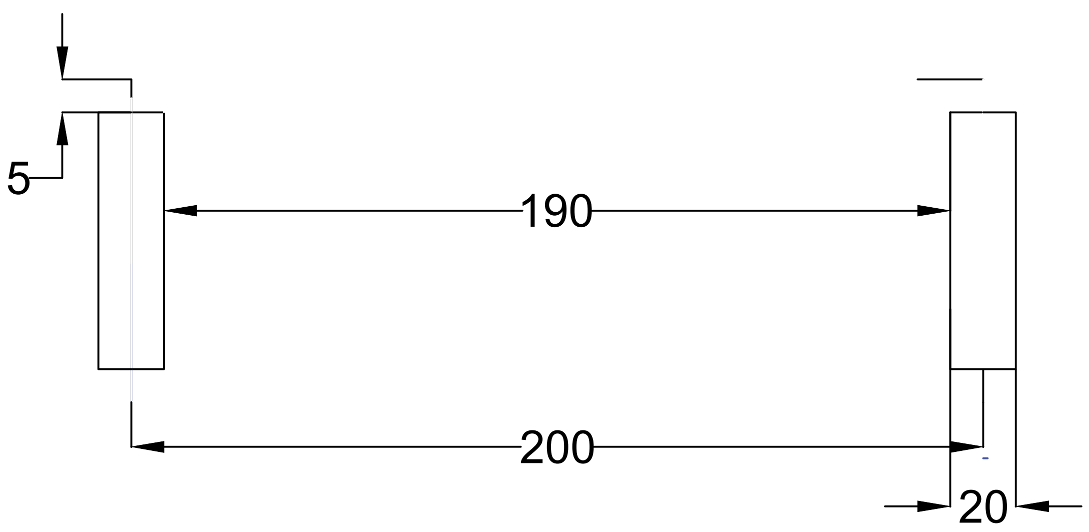

SAND BOX AND RIBS
(2.5 MM PLEXIGLASS)

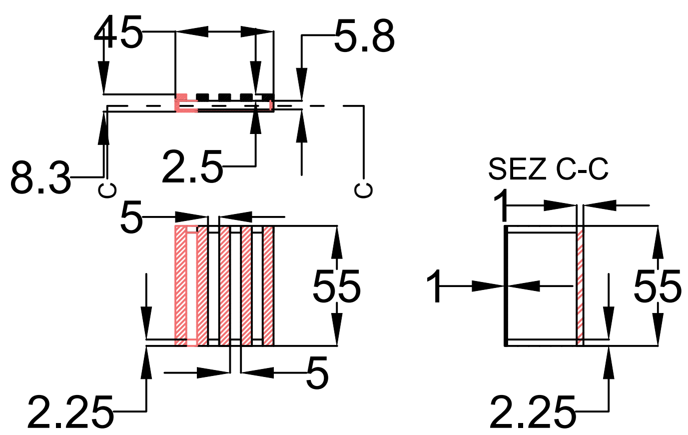

SANDTRAP

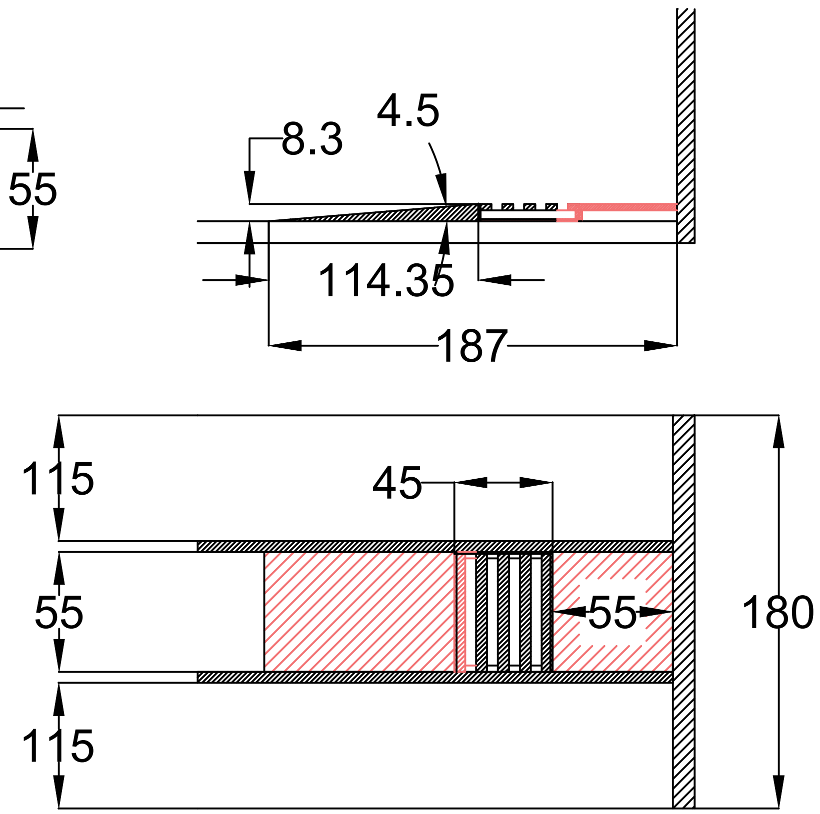

NTNU
Norwegian University of
Science and Technology